DEVELOPMENT OF DNA APTAMERS BY CELL-SELEX USING YEAST CELL SURFACE DISPLAY

A Dissertation

Presented to the Faculty of the Graduate School

of Cornell University

In Partial Fulfillment of the Requirements for the Degree of

Doctor of Philosophy

by

Hsien-Wei Meng

January 2014

© 2014 Hsien-Wei Meng

DEVELOPMENT OF DNA APTAMERS BY CELL-SELEX USING YEAST CELL SURFACE DISPLAY

Hsien-Wei Meng, Ph. D.

Cornell University 2014

SELEX, the process of selecting aptamers, is often hampered by the difficulty of preparing target molecules in their native forms and by a lack of a simple yet quantitative assay for monitoring enrichment and affinity of reactive aptamers. In this study, I established a new method to seek to discover DNA aptamers against human serum markers for potential therapeutic and diagnostic applications. To circumvent soluble expression and immobilization for performing SELEX, I ectopically expressed soluble growth factors on the surface of yeast cells to enable cell-SELEX and devised a flow cytometry-based method to quantitatively monitor progressive enrichment of specific aptamers. High-throughput sequencing of selected pools revealed that the emergence of highly enriched sequences concurred with the increase in the percentage of reactive aptamers shown by flow cytometry. I first tested if the yeast-surface display works as a platform for examining bindings of aptamers to target proteins. Afterwards, I particularly selected DNA aptamers against VEGF were specific and of high affinity (K_D = ~ 1 nM), and demonstrated a potent inhibition of capillary tube formation of endothelial cells, comparable to the effect of a clinically approved anti-VEGF antibody drug, bevacizumab. I also have successfully selected DNA aptamers

against PDGF-A, PDGF-B. Considering the fact that many mammalian secretory proteins have been functionally expressed in yeast, the strategy of implementing cell-SELEX and quantitative binding assay can be extended to discover aptamers against a broad array of soluble antigens.

BIOGRAPHICAL SKETCH

Hsien-Wei (Yvonne) Meng is the oldest child born to a Taiwanese family between Chao-Yi Meng and Li-Wen Tao in Nantou, Taiwan in February of 1984. Both of her parents are teachers in junior high schools in Nantou, so education is very important to the Meng family. She finished her Bachelor degree of Science in Life Sciences from National University of Kaohsiung. When she was in university, she worked as an undergraduate research assistant in Dr. Chun-Shun Wang's lab where she established the basic techniques in molecular biology and studies about Noda Virus (NNV) infection in red snapper to characterized and purified Noda Virus (NNV) antibody.

After undergraduate study, she entered department of Biological Chemistry in Academia Sinia, Taiwan to work as a lab research assistant in Dr. Sin-Tak Chu's lab where she gained more experience in working in a research lab and determined herself to pursue her Ph.D. degree overseas. Her research in Academia Sinica was to focus on female reproduction in the physiology of uterine inflammation and cancer in a mouse model of ectopic endometriosis surgically. During the two-year period at Dr. Chu's lab, she published several abstracts and presented at conferences, and contributed as an authorship in a peer reviewed journal paper.

She came to America to study her Ph.D. degree in Cornell University. Advised by Professor Moonsoo Jin during her PhD studies, Hsien-Wei had the opportunities to participate in a variety of research collaborations with other research labs in different fields. These interactions exposed her to valuable experience to work with experts from different academic backgrounds, and brought her useful materials and abundant

inspirations for research. Her research in Ph.D. is about developing a new strategy for cell-SELEX with yeast surface display system to select DNA aptamers and the work has been organized to a research paper and submitted to a journal. Hsien-Wei is passionate about starting her career in science and biotech, where she aims to develop more discovery and better products to people.

Dedicated to my husband, mom and dad, and to my two younger sisters.

For their constant love and support.

ACKNOWLEDGMENTS

I would like to gratefully and sincerely thank Dr. Moonsoo Jin for his guidance, understanding, patience, and most importantly, his friendship during my graduate studies at Cornell University. His mentorship was paramount in providing a well rounded experience consistent my long-term career goals. He encouraged me to not only grow as an experimentalist and a scientist but also as an instructor and an independent thinker.

I would also like to thank my committee members, Drs. John Lis, Scott Coonrod, and Holger Sondermann for all the help they have provided during my training. I am also indebted to Drs. Peter Doerschuk and David Lin for all the encouragements and cheers I have had. I would like to extend a special thank you to Belinda, Jenna, Arla for the superfast administrative support and the warmest welcomes whenever I dropped by their offices either in Weill Hall or in the Vet school.

I would also like to thank all of the members of the Jin research group, Goose, Zoe, Rich, Spencer, Fai, Turner, Tanwi, Yogi, Keon Woo, Xuebo, Ling, Taehyun, Ada, Kevin, Ester, Tricia, and especially Yoshiko and Karen for giving me the opportunity to act as a mentor to two excellent undergraduate students. These two friends and co-workers also provided for some much needed humor and entertainment in what could have otherwise been a somewhat stressful laboratory environment.

I would also like to thank our neighbors ,the Shen Lab and the Fischbach lab, for always generously sharing reagents and equipments with me, and also Pengcheng, Lihua, Yitian, Nikolai, Green, Jiahe, Bo Ri, Young Hye for their friendship and discussions that always inspired me a lot.

I would also like to thank every member in the Aptamer Community of Cornell University for their time, support, experimental discussions, and the valuable bi-weekly aptamer meetings (now happens once every month). I am especially grateful for Abdullah John, Kylan, and Li's friendship and all the puzzlings over many of the same problems. I would like to thank the Department of Biomedical Sciences and Department of Biomedical Engineering at Cornell University for all the shared equipments, and the department of Core Facility for the high-throughput sequencing work.

Finally, and most importantly, I would like to thank my husband Wayne. His support, encouragement, quiet patience and unwavering love were undeniably, and his unconditional love in the past few years of my life have been built. His tolerance of my occasional vulgar moods is a testament in itself of her unyielding devotion and love. I thank my parents and sisters in Taiwan for their faith in me and allowing me to be as ambitious as I wanted. It was under their watchful eye that I gained so much drive and an ability to tackle challenges head on. Also, I thank Wayne's family for their unending encouragement and support.

Most importantly, I thank God for His grace and love that protect and watch over me through my entire Ph.D. life.

TABLE OF CONTENTS

BIOGRAPHICAL SKETCH iii

DEDICATIONS. v

ACKNOWLEDGMENTS vi

TABLE OF CONTENTS viii

LIST OF FIGURES xii

LIST OF TABLES xviii

LIST OF ABBREVIATIONN xix

LIST OF SYMBOL xxi

CHAPTER 1 1

Cancer and Growth Factors. 1

Angiogenesis and Cancer 5

Therapeutic Strategies Related to Growth-Factor Inhibitors for Cancers 9

Aptamers 11

Aptamer and Antibodies 13

Organization of the dissertation 14

REFERENCES 17

CHAPTER 2 22

Summary 22

Introduction and Significance 22

Experimental Procedures 26

Procedure for yeast cell-SELEX 26

Flow cytometry for detecting antigen expression and aptamer binding in yeast 27
High-throughput DNA Sequencing 28
Results 28
Validate the feasibility of YSD as a novel platform of cell-SELEX. 29
Establish a novel platform for multiplexed-yeast-cell SELEX by using YSD to isolate specific aptamers. 32
Discussion 39
REFERENCES 42
CHAPTER 3 46
Summary 46
Introduction and Significance 47
Experimental Procedures 49
Procedure for yeast cell-SELEX. 49
Flow cytometry for detecting antigen expression and aptamer binding in yeast. 50
Flow cytometry for measuring VEGF binding to HeLa cells. 51
High-throughput DNA Sequencing. 52
Gel-shift assay with fluorescein-labeled aptamer. 52
Human umbilical vein endothelial cell (HUVEC) capillary tube formation assay. 53
Results 53
Cell-SELEX implemented by ectopic expression of human growth factors

on yeast cell surface. 53
Discovery of specific aptamers in accordance with the degree of sequence multiplicity. 57
Identification and characterization of aptamers for VEGF. 60
Aptamers bind the heparin-binding domain in VEGF. 65
hVaps potently inhibit capillary tube formation of endothelial cells. 69
Discussion 72
SUPPLEMENTARY MATERIALS 77
REFERENCES 81
CHAPTER 4 85
Conclusions 85
Future Directions 86
Aptamer as imaging probes. 87
Aptamer as therapeutics 88
REFERENCES 89
APPENDIX 1 91
Summary 91
Introduction and Significance 92
Experimental Procedures 94
Transfection 94
Immunofluorescence Flow Cytometry. 95
Results 95
The design of Anchored-I domain 95

Characterization of Fc-AncId-HA protein in mammalian-cell system 96

Discussion..... 100

REFERENCES..... 102

LIST OF FIGURES

Figure 1-1. The stepwise progression of cancer and roles for growth factors. 1

Figure 1-2. A, Tumor cells produce VEGF-A and other angiogenic factors such as bFGF, angiopoietins, interleukin-8, and VEGF-C. These stimulate resident endothelial cells to proliferate and migrate. B, An additional source of angiogenic factors is the stroma cells. This is a heterogeneous compartment, comprising fibroblastic, inflammatory and immune cells. VEGF-A or PlGF may recruit bone-marrow-derived angiogenic cells (BMC). Tumor cells may also release stromal-ell-recruitment factors, such as PDGF-A, PDGF-C or transforming growth factor β (TGF-β). A well-established function of tumor-associated fibroblasts is the production of growth/survival factor for tumor cells such as EGFR ligands, hepatocyte growth factor and heregulin. C Endothelial cells produce PDGF-B, which promotes recruitment of pericytes in the microvasculature after activation of PDGFR-β. 8

Figure2-1. Verification of cell-SELEX with yeast surface display system. (a) Dissociation constant (Kd) measurement from flow cytometry. The binding affinity of Pap1 measured by flow cytometry assay is 27.3 nM. The formula that calculated Kd equals to $[ssDNA]_{1/2\ Fluorescence(Max)}$. (b) The design of biotinylated capturing oligo coupling to streptavidin-PE. (c) Binding of Pap1 and anti-c-myc/ anti-HA antibody to yeast before (shaded) and after (solid line) target protein expressed on the surface. 31

Figure 2-2. Characterization of Multiplexed-Yeast Cell SELEX. (a). Schematic flow of DNA aptamer selection using the yeast-cell SELEX. (b). Monitoring the progress of yeast-cell SELEX from R0 to R8. The histograms are showing detections of target screened libraries, known aptamers, and anti-c-myc antibody to yeast before (shaded) and after (thick lines) target protein expressed on the surface. (c). Binding test of newly selected aptamers of PDGF-BB to yeast before (shaded) and after (thick lines) target protein expressed on the surface. 35

Figure 3-1. Cell-SELEX procedure implemented by ectopic expression of human soluble growth factors on yeast cell surface. (a) A schematic drawing illustrates the procedure for cell-SELEX. Each round consists of subtractive panning, PCR amplification, and recovery of aptamer sequences by lambda exonuclease digestion. Human soluble growth factors were displayed on yeast cell surface as a fusion to agglutinin, composed of Aga1p and Aga2p subunits. Surface expression of the protein of interest was confirmed by antibody binding to hemagglutinin (HA) tag (YPYDVPDYA) and c-myc (EQKLISEEDL) tag. Enrichment and affinity of reactive aptamers to target molecules were quantified by flow cytometry. Selected aptamer pools were subjected to high throughput sequencing to isolate highly enriched sequences. (b) Aptamers for flow cytometry experiments were captured by biotinylated oligonucleotides complementary to either 5’ or 3’ constant regions. This DNA complex was mixed with PE-conjugated

streptavidin at a 1:1 molar ratio. (c) Progressive enrichment of reactive aptamers against PDGF-A, VEGF, and IL-6 were confirmed by flow cytometry. Shown are the binding of aptamers to unrelated proteins (PDGF-B or EGFR) drawn in shaded histograms or to target proteins in open histograms. The percentage of subpopulations defined by arrows is shown for each histogram. Aptamers were used at 200 nM. 56

Figure 3-2. Confirmation of binding specificity of the top-ranked aptamers identified by sequence multiplicity. Highly enriched aptamer sequences were identified by high-throughput sequencing analysis, and tested by flow cytometry for specificity and binding affinity to respective targets. The binding of individual aptamers to respective target is shown as open histograms drawn in thick line, to unrelated protein as open histograms in thin line, and to uninduced yeast cells as closed histograms. The percentage of subpopulations defined by arrows is shown for each histogram. 58

Figure 3-3. Determining consensus motif, secondary structure, and solution affinity of the aptamers against VEGF. (a) The consensus motif shared among the top ten highly enriched sequences against VEGF was identified using the MEME Suite (http://meme.nbcr.net/meme/). (b) Shown are the secondary structures of the 60-nt variable region of the top two aptamers, hVap1 and hVap2, predicted by Mfold (http://mfold.rna.albany.edu/). (c-d) Solution affinity (K_D) of the full-length hVap1 and hVap2 against VEGF was determined by F-EMSA

(c), and by fitting the Hill equation to the data (d). VEGF was used at a series of 2/3-fold serial dilutions starting at 53 nM, while labeled aptamers were used at 500 pM. 61

Figure 3-4. Identification of structural motifs of anti-VEGF aptamers. (a) Full-length anti-VEGF aptamers were shortened to contain the first stem-loop containing the consensus motif shared among all highly sequenced aptamers and a part of the longer stem-loop. (b-c) The binding affinities of all four truncated aptamers were determined by F-EMSA assay (b) and by curve-fitting of the Hill equation to the data (c). VEGF was used at a series of 2/3-fold dilutions starting from 500 nM, and labeled aptamers were at 600 pM. 64

Figure 3-5. Selected aptamers bind the HBD in VEGF. (a) The potency of anti-VEGF aptamers for the inhibition of VEGF binding to VEGFR was measured as the percent inhibition of VEGF binding to VEGFR-expressing HeLa cells. VEGF at 250 nM was pre-incubated with hVap2 at 0 - 250 nM. VEGF binding to cells was detected by polyclonal anti-VEGF antibody. (b) Anti-VEGF aptamers were tested for binding to yeast cells expressing VEGF165 or VEGF110 lacking in HBD with or without post-incubation with 100 nM heparin. Heparin was used to compete with the aptamers for binding to VEGF. VEGF expression was confirmed by polyclonal anti-VEGF antibody. Truncated aptamers were biotinylated at the 5’ end to form a complex with PE-conjugated streptavidin. (c) Sequence alignment of human (H) and murine (M)

VEGF. '*' indicates identical amino acids between human murine VEGF. Receptor binding domain (residues 1-110 for human VEGF) and heparin binding domain (residues 111-165 for human VEGF) are denoted. (d) Comparison of the level of binding of hVap1 and hVap2 to human (shown in thick open histograms) and murine VEGF (shown in thin open histograms). Aptamer binding to uninduced yeast cells is shown in filled histograms. Aptamers were bound with the biotinylated oligonucleotides complementary to the 5' constant region to form a complex with PE-conjugated streptavidin. 68

Figure 3-6. Anti-VEGF aptamers antagonize angiogenesis. Antagonistic potency of anti-VEGF aptamers was measured by a capillary tube formation assay using HUVECs embeded in Matrigel. (a) Shown are the representative images of HUVECs forming capillary tubes after HUVECs were cultured in the presence of anti-VEGF aptamers, bevacizumab, and various controls. Scale bar = 100 μm. (b) Total tube length within a randomly chosen microscopic field (25x magnification) was quantified by Angiogenesis Analyzer for ImageJ software. Bar graph shows the mean and standard deviation of the measured total tube length (n = 3). 71

Figure A-1. Characterizations of I domain fusion proteins. 96

Figure A-2. Newly engineered AncId-HA can be functionally expressed in mammalian cell system and in yeast-surface display system. (a). Fc-AncId-HA was constructed in vector pHIV and successfully expressed

in Hela cells with the fusing EGFP expressed. (b) AncId-HA was constructed in vector pNL6, and the yeast cells show binding interaction with Hela cells. Yeast cells appear as small bright spheres in the images. 99

Figure A-3. Comparison of binding affinity to ICAM-I. Wildtype Id yeast, αL Id-HA yeast, and AncId-HA yeast were used to test the binding with 9E10, TS1/22, and rhICAM-1/Fc. Though AncId-HA yeast didn't show binding to TS1/22, it shows the strongest binding to rhICAM-1/Fc. 100

LIST OF TABLES

Table 2-1. Enriched aptamer sequences selected against PDGF-BB. 38

Table 3-1. Enriched aptamer sequences selected against target molecules.. 59

Table 3-2. Nucleotide sequences of truncated hVaps 65

LIST OF ABBREVIATIONN

Abbreviation	Meaning
5-IAF	5-iodoacetamidofluorescein
APBB	Aptamer binding buffer
B-CO	Biotinylated capturing oligos
BMC	Bone-marrow-derived angiogenic cells
DTT	Dithiothreitol
dsDNA	Double-strand dna
EMSA	Electrophoretic mobility shifted assay
ER	Endoplasmic reticulum
EPCs	Endothelial progenitor cells
EGF	Epidermal growth factor
EPO	Erythropoietin
Flk-1	Fetal liver kinase 1
F-EMSA	Fluorescence electrophoretic mobility shift assay
FP	Fluorescence polarization
GFs	Growth factors
HA	Hemagglutinin
HBD	Heparin-binding domain
HUVECs	Human umbilical vein endothelial cell
IGF-1	Insulin-like growth factor 1
ICAM-I	Intercellular adhesion molecule 1

IL-8	Interleukin 8
KDR	Kinase insert domain receptor
mTOR	Mammalian target of rapamycin
MMPs	Metalloproteinases
M-SELEX	Microfluidic selex
mM	Millimolar
MI	Molecular imaging
nM	Nanomillar
PBS	Phosphate buffered saline
PCR	Polymerase chain reaction
hPAap	PDGF-A aptamer
Pap	PDGF-BB aptamer
PE	Phycoerythrin
PDGF	Platelet-derived growth factor
RTKs	Receptor tyrosine kinases
SELEX	Systematic evolution of ligands by exponential enrichment
ssDNA	Single-strand dna
SPR	Surface plasmon resonance
TGF-β	Transforming growth factor beta
TNF-α	Tumor necrosis factor alpha
VEGF	Vascular endothelial growth factor
YSD	Yeast surface display

LIST OF SYMBOL

Symbol	Variable or parameter	Dimensions
K_D	equilibrium dissociation constant	nM

CHAPTER 1

INTRODUCTION

Cancer and Growth Factors.

Cancer refers to a group of different diseases which are characterized by abnormal growth and spread of malignant cells. The causes of cancer are multifaceted, arising from both internal and external factors, which result in detrimental alteration of normal gene expressions and/or protein expressions. These phenomena cause cells to obtain increasingly abnormal proliferation and invasion. For instance, induction of uncontrolled cell growth leading to cancer can occur when the protein expression levels or post-translational modification patterns are altered and/or when there is an incidence of genetic abnormality [1].

In physiological conditions, cells receive fate-determining signals from the surrounding tissues, primarily in the form of polypeptide growth factors. The foundation and the first building block of tissue homeostasis is the organized integration of these extracellular signals. After the departure and float from homeostasis, tumor initiations are associated with oncogenic mutations. Afterwards, growth factors are the major regulators of all subsequent steps of tumor progression and invasion, namely metastasis, invasion across tissue barriers, angiogenesis, and colonization of distant locations [2]. Angiogenesis is the formation of new blood vessels. This process involves the migration, growth, and differentiation of endothelial

cells which line the inside wall of blood vessels. Angiogenesis plays a critical role in the growth and spread of cancer. A blood supply is necessary for tumors to grow beyond a few millimeters in size. Tumors can cause this blood supply to form by giving off chemical signals that stimulate angiogenesis. Tumors can also stimulate nearby normal cells to produce angiogenesis signaling molecules. The resulting new blood vessels "feed" growing tumors with oxygen and nutrients, allowing the cancer cells to invade nearby tissue, to move throughout the body, and to form new colonies of cancer cells, called metastases.

Once initiated by driver mutations, pre-malignant epithelial cells may accumulate additional oncogenic mutations, but their expansion and progression to metastatic carcinomas depend on a multi-step process orchestrated primarily by growth factors (GFs) (Figure 1-1). The multi-step process contains: 1) Driver mutation, 2) Clonal expansion, 3) Carcinoma in situ or intraepithelial neoplasia, 4) Invasion, 5) Dissemination, 6) Micrometastases, 7) Resistant clones after chemotherapy or radiotherapy, 8) Angiogenesis, and 9) Metastasis. GFs are polypeptides [3] bind to transmembrane receptors mediating kinase activity [4] to stimulate specific combinations of intracellular signaling pathways [5-7]. These cellular activations and the respective GFs are co-opted in several phases of tumor progression [8]. The metastatic process enables GFs to support tumor progression [9, 10].

1

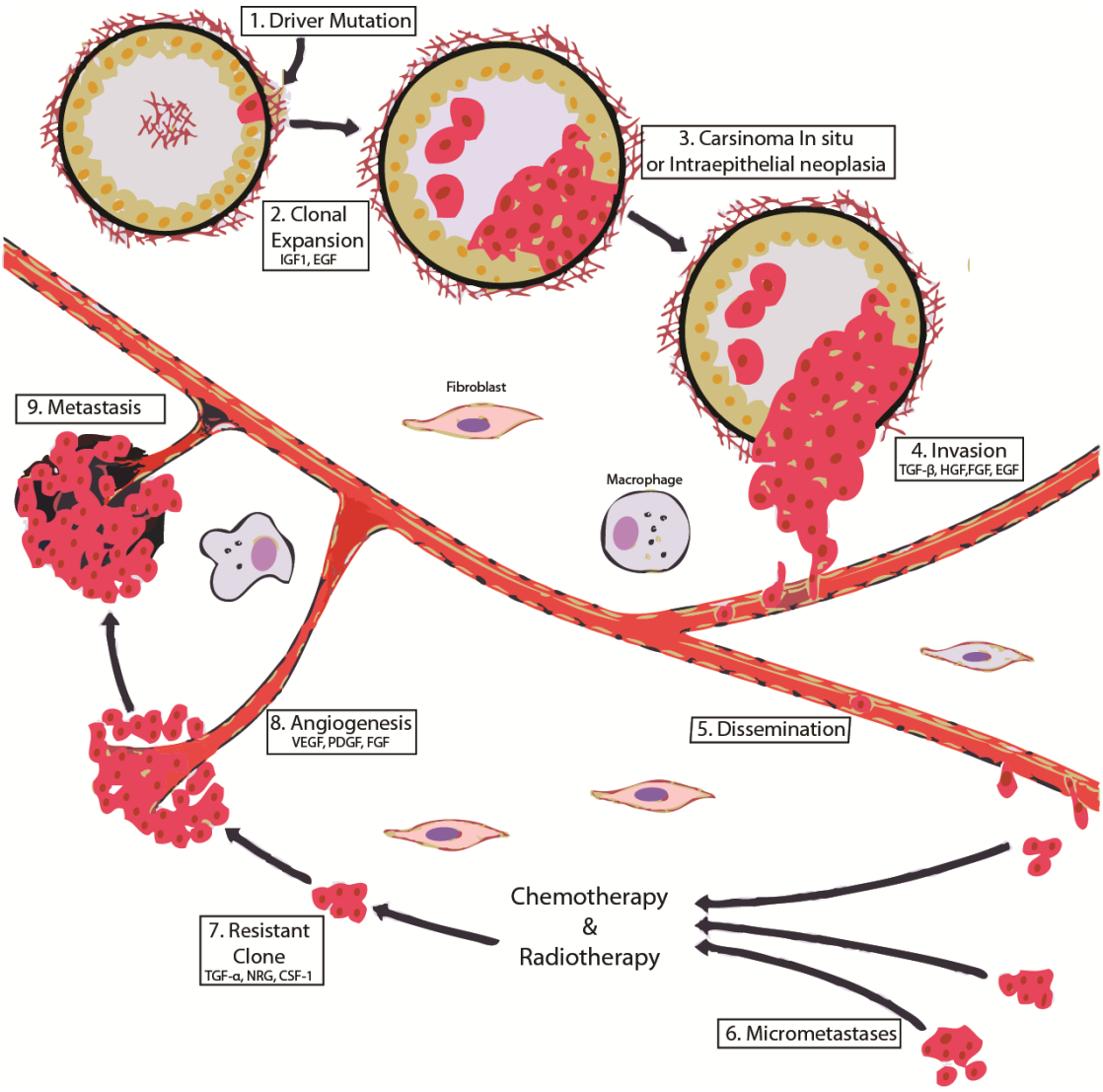

[1] This figure is modified and reproduced from the article originally published in Physiology (Esther Witsch, Michael Sela, and Yosef Yarden. *Physiology (Bethesda).* 2010 April; 25(2): 85–101.

Figure 1-1. The stepwise progression of cancer and roles for growth factors.
The process is initiated by a somatic mutation that gives considerable survival and growth advantages to the initiated cell (Step 1). GFs such as Epidermal Growth Factor (EGF) and Insulin-like Growth Factor 1(IGF1) support the followig expansion of mutation-bearing clones (Step 2), and the event usually leads to intraluminal lesions (Step 3), such as carcinoma in situ or intraepithelial neoplasia, which are surrounded by the basal membrane. Invasion (Step 4) refers to the migration and penetration into neighboring tissues of cancer cells. Cancer cells enter (extravasation) and exit (intravasation) lymphatic and blood vessels to disseminate (Step 5) and metastasize to distant organs or tissues. Extra- and intravasation entail the supporting functions of macrophages, platelets, and endothelial cells. The resulting micrometastases (Step 6) are usually sensitive to chemotherapy and radiotherapy. However, the new mutations and the ability of cancer cells to produce GFs (autocrine loops) improve the growth of resistant clones (Step 7). Angiogenesis (Step 8) is essential for the establishment of secondary tumors. Both sprouting of existing vessels and recruitment of bone marrow-derived endothelial progenitor cells are stimulated by GFs secreted by tumor and stromal cells. At the final stage, relatively large metastases (Step 9) populate a definite set of target organs. Note that a latency period of several years may precede this final phase.

Tumor cells have an absolute requirement for a persistent supply of new blood vessels to nourish their growth and to facilitate metastasis. Thus, tumor vascularization is a pivotal process for the progression of a neoplasm from a small localized tumor to an enlarging tumor with the ability to metastasize [11]. The growth of human tumors and development of metastases depend on the de novo formation of blood vessels. The formation of new blood vessels is tightly regulated by specific growth factors that target receptor tyrosine kinases (RTKs)[12]. Vascular endothelial growth factor (VEGF), Platelet-derived growth factor (PDGF), and the Fetal Liver Kinase 1 (Flk-1)/ Kinase insert domain receptor (KDR) RTK have been implicated as the key endothelial cell-specific factor signaling pathway required for pathological angiogenesis, including tumor neo-vascularization [12].

Angiogenesis and Cancer

The generation of new vessels is critical for tumor growth beyond few millimeters of size. New vessels are formed either by mature endothelial cells (angiogenesis)[13] or by bone marrow-derived endothelial progenitor cells (EPCs)[14], which are home to foci of angiogenesis (vasculogenesis)[15]. Growth factors like the vascular endothelial growth factors (VEGFs), FGFs [16], and TGF-β play important roles in both vasculogenesis and angiogenesis, and VEGF antagonists limit angiogenesis in animals and in patients. EPCs regulate the angiogenic switch via paracrine secretion of proangiogenic growth factors and by direct luminal incorporation into sprouting nascent vessels [17]. Mobilization of circulating

progenitors and other endothelial cells to tumors emerges as a critical step in tumor progression.

Transcription level of VEGF mRNA is also induced by different growth factors and cytokines, including PDGF, EGF, tumor necrosis factor alpha (TNF-α), and interleukin 1-beta [18, 19]. The initial step of transcription induced by hypoxia in tumor growth and factor secretion by the growing tumor and the stromal tissue leads to an upregulation and activation of growth factor receptors. Results in endothelial sprouting, increased vascular permeability, the expression of tissue matrix metalloproteinases (MMPs), and eventually the digestion of matrix, which is required for the endothelial cell to move [12]. The increased mitogenesis of endothelial cell and spread and activation of other factors lead to the formation and travel of endothelial cells, including other supporting cells, and eventually lead to vessel extension, increased capillary integrity, differentiation of micro-vessel support cells, and formation of the vascular network. VEGF plays a role in the earliest events in this process.

The PDGF signaling system has been proven that it contributes to tumor angiogenesis and vascular remodeling. In the study of Xue et. al. [20] suggested that PDGF-BB–induced erythropoietin (EPO) promotes tumor growth through two mechanisms: 1) paracrine stimulation of tumor angiogenesis by direct induction of endothelial cell proliferation, migration, sprouting and tube formation, and 2) endocrine stimulation of extramedullary hematopoiesis by inducing erythropoietin production in stromal cells leading to increased oxygen perfusion and protection against tumor-associated anemia (Figure 1-2).

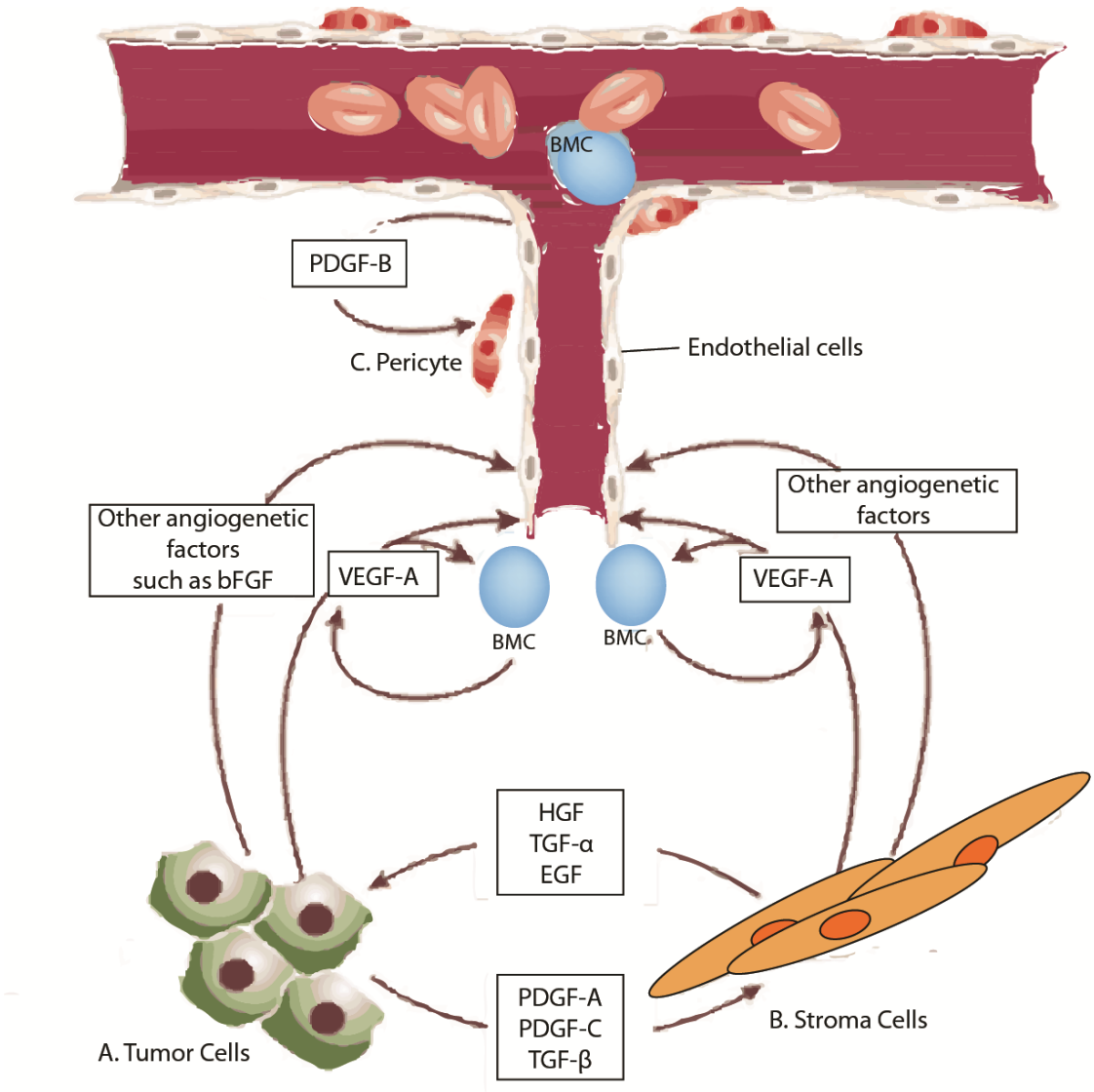

2

[2] This figure is modified and reproduced from the article originally published in *Nature* (Napoleone Ferrara & Robert S. Kerbel. *Nature*. 2005 **438**, 967-974).

Figure 1-2. A, Tumor cells produce VEGF-A and other angiogenic factors such as bFGF, angiopoietins, interleukin-8, and VEGF-C. These stimulate resident endothelial cells to proliferate and migrate. B, An additional source of angiogenic factors is the stroma cells. This is a heterogeneous compartment, comprising fibroblastic, inflammatory and immune cells. VEGF-A or PlGF may recruit bone-marrow-derived angiogenic cells (BMC). Tumor cells may also release stromal-ell-recruitment factors, such as PDGF-A, PDGF-C or transforming growth factor β (TGF-β). A well-established function of tumor-associated fibroblasts is the production of growth/survival factor for tumor cells such as EGFR ligands, hepatocyte growth factor and heregulin. C Endothelial cells produce PDGF-B, which promotes recruitment of pericytes in the microvasculature after activation of PDGFR-β.

In the gene expression level, Westphal *et. al.* have studied the expression of a panel of angiogenic factors, and of the angiogenesis inhibitor angiostatin, in a panel of human melanoma cell lines giving rise to xenografts with different vascular densities [21]. In their study, expression of basic fibroblast growth factor (bFGF) and VEGF was clearly correlated with a high degree of vascularization, confirming the importance of these factors for tumor angiogenesis [21]. In addition, there was exclusive or elevated in vitro expression of angiogenic factors interleukin 8 (IL-8), PDGF-AB, and, to a lesser extent, midkine in cell lines that formed highly vascularized tumors. A similar angiogenic-factor-expression pattern was found in the corresponding xenografts, with the exception of VEGF. In most cell lines, this factor had low expression in vitro which was strongly enhanced in vivo [21].

From the above, every study provides evidence for the notion that regulation of tumor angiogenesis is dependent on multiple factors. Inhibition of angiogenesis for therapeutic purposes, therefore, should preferably not concentrate on a single factor.

Therapeutic Strategies Related to Growth-Factor Inhibitors for Cancers

The process of angiogenesis is controlled by chemical signals of growth factors in the body. These signals can stimulate both the repair of damaged blood vessels and the formation of new blood vessels. There are other chemical signals called angiogenesis inhibitors interfere with blood vessel formation[22]. Normally, the stimulating and inhibiting effects of angiogenic signals are regulated and balanced so that blood vessels form only when and where they are needed[23]. Pathological

angiogenesis is a hallmark of cancer and various ischaemic and inflammatory diseases[24]. To progress, angiogenesis is essential for tumor growth and metastasis, controlling tumor-associated angiogenesis is an effective method in limiting cancer progression and invasion. The tumor micro-environment comprises numerous signaling molecules and pathways that regulate the angiogenic response. Understanding how these components functionally interact to each other as angiogenic triggers or as suppressors and how the mechanisms of resistance arise is required for the identification of new therapeutic strategies. Growth blockers (also called cancer growth inhibitors) are a type of biological therapy and include tyrosine kinase inhibitors, proteasome inhibitors, mammalian target of rapamycin (mTOR) inhibitors, phosphoinositide 3-kinase (PI3K) inhibitors, histone deacetylase inhibitors and hedgehog pathway blockers. Achieving a durable and efficient anti-angiogenic response will require approaches to simultaneously or sequentially target multiple aspects of the tumor microenvironment[25]. Because tumors cannot grow beyond a certain size or spread without a blood supply, scientists are trying to find ways to block tumor angiogenesis. They are studying natural and synthetic angiogenesis inhibitors, also called anti-angiogenic agents, with the idea that these molecules will prevent or slow the growth of cancer.

Inhibition of the VEGF tyrosine kinase signaling pathway blocks new blood vessel formation in growing tumors, leading to stasis or regression of tumor growth[12]. Advances in understanding the biology of angiogenesis have led to the development of several therapeutic modalities for the inhibition of the VEGF tyrosine kinase signaling pathway. A number of these modalities are under investigation in

clinical studies to evaluate their potential to treat human cancers. Such as SU5416, a novel synthetic compound, is a potent and selective inhibitor of the Flk-1/KDR receptor tyrosine kinase that is presently under evaluation in Phase I clinical studies for the treatment of human cancers[26]. Clinically, there are several effective cancer drugs are targeting VEGF and PDGF receptor tyrosine kinase signaling. Bevacizumab, an anti-VEGF antibody for treating cancer, has been commonly used for treating patients with first-line therapy for metastatic colorectal cancer[27]. Sorafenib, a multikinase inhibitor, targets both Raf and VEGF and PDGF receptor tyrosine kinase signaling have been developed and studied clinically[28]. CP-673,451 is a potent inhibitor of platelet-derived growth factor β-receptor (PDGFR-β) kinase- and PDGF-BB-stimulated autophosphorylation of PDGFR-β in cells (IC50 = 1 nmol/L) being more than 450-fold selective for PDGFR-β versus other angiogenic receptors (e.g., vascular endothelial growth factor receptor 2, TIE-2, and fibroblast growth factor receptor 2)[29]. Pegaptanib sodium (Macugen), an anti-vascular endothelial growth factor (anti-VEGF) RNA aptamer, for the treatment of all types of neovascular age-related macular degeneration (AMD)[30]. Thus, it is important to understand the physiology of VEGF and PDGF and their receptors as well as their roles in malignancies in order to develop antiangiogenic strategies for the treatment of malignant disease.

Aptamers

Aptamers are specific DNA or RNA short-oligonucleotides that have been

isolated from large random sequence pools for their ability to bind specific target molecules. Aptamers are selected via an iterative in vitro process called SELEX (Systematic Evolution of Ligands by EXponential enrichment) [31-33]. A typical SELEX round contains the following three steps:1) Binding: incubation of the library with the target, 2) Partitioning: separation of target-bound library sequences from unbound ones, 3 Amplification: generation of a new and selected pool of nucleic acids by making multiple copies of the sequences that bound to the target. These steps are then repeated in an iterative fashion to obtain an enriched pool and the target binding aptamers are identified via cloning and sequencing processes. After successful selections of aptamers, aptamers are cloned and individually sequenced. In recent years, the conventional SELEX approach has been significantly improved in reducing laborious handlings in several different manners; however, the selection of aptamers to multiple targets in parallel is not well established. Also, the laborious purification of target proteins at the beginning stage and cloning to sequence individual aptamers at the last step remain to be tedious. Selection of specific aptamers to intact cells, cell-SELEX, was first achieved in 1997[34]. In cell-SELEX, SELEX methodology is used with a complex mixture of cells as potential targets. Ligands to multiple targets are generated simultaneously during the selection process, and the binding affinities of these ligands for their targets are comparable to those found in similar experiments against pure targets. The approach was originally designed for when the clear marker target is unknown; so far, live cells of different cancers have been used in this process. With the FDA-approved drug Pegaptanib sodium (Mucagen) now available, others, such as AS1411, (nucleolin aptamer in clinical trial)[35], aptamers will contribute

immensely in cancer therapy.

Aptamer and Antibodies

Being very alike to antibodies, aptamers can bind with high affinity and specificity to target molecules ranging from proteins to small peptides [36, 37]. Based on their capabilities of target recognition, selective binding, and affinity, aptamers have been likened to antibodies. However, aptamers, by their unique features, have more flexibility in their development and range of applications. Specifically, aptamers can be generated using a variety of conditions, and the time needed for the generation of aptamers by the SELEX process is relatively short. Moreover, the use of animals for antibody production can lead to batch–to-batch variation. However, aptamers are chemically synthesized, which eliminates the possible batch-to-batch variations associated with antibodies. Furthermore, chemical synthesis of aptamers permits the biochemical manipulation required to incorporate various functional groups and specific moieties without compromising the function of most aptamers. This phenomenon has been adopted for aptamer conjugation with drug molecules and nanomaterials and for the modification of nuclease resistance bases, such as locked nucleic acids and 2‘-O-methyl nucleotide analogues, to further enhance nuclease resistance when adopted for in vivo study[38, 39]. Other comparable qualities, such as long-shelf life, controllable or cyclical denaturation, and renaturation, have expanded the flexibility of aptamers in various experimental designs. Even with improved nuclease resistance, aptamers have low blood residence times compared to antibodies,

as well as low toxicity or immunogenicity (if any), and these are important features when used for in vivo applications such as imaging. The demand for diagnostic assays to assist in the management of existing and emerging diseases is increasing, and aptamers could potentially fulfill molecular recognition needs in those assays. Compared with the bellwether antibody technology, aptamer research is still in its infancy, but it is progressing at a fast pace. The potential of aptamers may be realized in the near future in the form of aptamer-based diagnostic products in the market. In such products, aptamers may play a key role either in conjunction with, or in place of, antibodies. It is also likely that existing diagnostic formats may change according to the need to better harness the unique properties of aptamers[40].

Organization of the dissertation

In the dissertation, I proposed to develop a multiplex cell-SELEX by using yeast surface display (YSD) technique that will be used to select aptamers in parallel to many proteins, with the initial target protein set including splice variants and differently post-translationally modified versions of the same proteins, as well as unrelated proteins with different physical properties and cellular associations, and with physiological and patho-physiological value. I have chosen a set of growth factors who have been proved played pivotal roles in pathological angiogenesis involved in cancer. Our goal is to obtain multiple DNA aptamers for each of these proteins. The selected aptamers will then be incorporated into high-throughput protein capture/detection assays using pairs of aptamers to detect each protein with high

specificity. Additionally, the aptamers will be tested for their inhibitory effects with the idea that some of the selected aptamers could be developed into inhibitory molecular drugs or used for validation of target proteins in therapeutic intervention. This dissertation has been expected to have major impact on a wide variety of medical and life sciences research, since the multiplex SELEX method will enable rapid selection of many aptamers against a large set of proteins in a cost-effective way. Moreover, the approaches could be used to focus on various large collections of specific medically-relevant marker, and potentially be scaled up to the entire proteome. The selected aptamers will not only be used to develop detection/capture reagents, but they can serve as inhibitors to study the function of the target proteins in vivo and to validate potential drug targets. An overview of the chapters and appendix are given below.

Chapter 1: Introduction. This chapter provides the background on current studies of cancer related growth factors, and the current strategies of cancer treatment established based on the importance of these growth factors. In this part, I also present the related knowledge that inspired our work (especially our preliminary studies on protein engineering, yeast-surface display systems, SELEX, and cell-SELEX), as well as an introduction to the overall content of this dissertation.

Chapter 2: Aptamer Discovery Using Yeast Display Cell-SELEX for Cancer Detection and Intervention. In this chapter, I described the development of the new method of yeast-cell SELEX incorporated with Yeast Surface Display (YSD) system. By using the known DNA aptamer of PDGF-BB, Pap1[41], I first demonstrated the YSD system can be served as a protein immobilization platform for binding of target-

specific aptamers. I also documented the pilot screening of yeast-cell SELEX with known DNA aptamers, PDGF-BB aptamer 1 (Pap1) and VEGF aptamer 7 (Vap7)[42], of PDGF-BB and VEGF-A spiked-in DNA aptamer library.

Chapter 3: Discovering Aptamers by Cell-SELEX against Human Soluble Growth Factors Ectopically Expressed on Yeast Cell Surface. This chapter was modified from a submitted publication to PLOS ONE and granted permission for being documented in the dissertation. In the chapter, I delivered a completed yeast-cell SELEX for multiple targets of growth factors with several new DNA aptamers discovered. By combining the results of yeast-cell SELEX with high-throughput sequencing technology, I have discovered the enrichment ratio and progression of yeast-cell SELEX can be monitored by flow cytometry, and the sequencing reads of each aptamer cluster from high-throughput sequencing showed strong correlation to its binding affinity to targets. At the same time, I have successfully created and identified a novel and high-affinity DNA aptamers to VEGF, and the aptamer have showed significant inhibition to tube (Human umbilical vein endothelial cell, HUVECs) formation assay which is a biologic experiment of angiogenesis.

Chapter 4: Conclusions and Future Work. This chapter provides an overall conclusion of the work presented in this dissertation, as well as suggestions for future research directions.

Appendix I: This chapter documents the engineering of β1 I-like domain, additional work I have accomplished along the efforts on engineering integrin α I domains.

REFERENCES

1. Jensen, O.N., Modification-specific proteomics: characterization of post-translational modifications by mass spectrometry. Curr Opin Chem Biol, 2004. 8(1): p. 33-41.

2. Witsch, E., M. Sela, and Y. Yarden, Roles for growth factors in cancer progression. Physiology (Bethesda), 2010. 25(2): p. 85-101.

3. Deuel, T.F., Polypeptide growth factors: roles in normal and abnormal cell growth. Annu Rev Cell Biol, 1987. 3: p. 443-92.

4. Ullrich, A. and J. Schlessinger, Signal transduction by receptors with tyrosine kinase activity. Cell, 1990. 61(2): p. 203-12.

5. Rieck, P.W., S. Cholidis, and C. Hartmann, Intracellular signaling pathway of FGF-2-modulated corneal endothelial cell migration during wound healing in vitro. Exp Eye Res, 2001. 73(5): p. 639-50.

6. Olayioye, M.A., Update on HER-2 as a target for cancer therapy: intracellular signaling pathways of ErbB2/HER-2 and family members. Breast Cancer Res, 2001. 3(6): p. 385-9.

7. Sweeney, C., et al., Growth factor-specific signaling pathway stimulation and gene expression mediated by ErbB receptors. J Biol Chem, 2001. 276(25): p. 22685-98.

8. Aaronson, S.A., Growth factors and cancer. Science, 1991. 254(5035): p. 1146-53.

9. Hanahan, D. and R.A. Weinberg, The hallmarks of cancer. Cell, 2000. 100(1):

p. 57-70.

10. Nguyen, D.X., P.D. Bos, and J. Massague, Metastasis: from dissemination to organ-specific colonization. Nat Rev Cancer, 2009. 9(4): p. 274-84.

11. Hayes, A.J., L.Y. Li, and M.E. Lippman, Anti-vascular therapy: a new approach to cancer treatment. West J Med, 2000. 172(1): p. 39-42.

12. McMahon, G., VEGF receptor signaling in tumor angiogenesis. Oncologist, 2000. 5 Suppl 1: p. 3-10.

13. Hoeben, A., et al., Vascular endothelial growth factor and angiogenesis. Pharmacol Rev, 2004. 56(4): p. 549-80.

14. Nolan, D.J., et al., Bone marrow-derived endothelial progenitor cells are a major determinant of nascent tumor neovascularization. Genes Dev, 2007. 21(12): p. 1546-58.

15. Asahara, T., et al., Isolation of putative progenitor endothelial cells for angiogenesis. Science, 1997. 275(5302): p. 964-7.

16. Cross, M.J. and L. Claesson-Welsh, FGF and VEGF function in angiogenesis: signalling pathways, biological responses and therapeutic inhibition. Trends Pharmacol Sci, 2001. 22(4): p. 201-7.

17. Gao, D., et al., Bone marrow-derived endothelial progenitor cells contribute to the angiogenic switch in tumor growth and metastatic progression. Biochim Biophys Acta, 2009. 1796(1): p. 33-40.

18. Neufeld, G., et al., Vascular endothelial growth factor (VEGF) and its receptors. FASEB J, 1999. 13(1): p. 9-22.

19. Ferrara, N. and T. Davis-Smyth, The biology of vascular endothelial growth

factor. Endocr Rev, 1997. 18(1): p. 4-25.

20. Xue, Y., et al., PDGF-BB modulates hematopoiesis and tumor angiogenesis by inducing erythropoietin production in stromal cells. Nat Med, 2012. 18(1): p. 100-10.

21. Westphal, J.R., et al., Angiogenic balance in human melanoma: expression of VEGF, bFGF, IL-8, PDGF and angiostatin in relation to vascular density of xenografts in vivo. Int J Cancer, 2000. 86(6): p. 768-76.

22. Ray, F.R., et al., Purinergic receptor distribution in endothelial cells in blood vessels: a basis for selection of coronary artery grafts. Atherosclerosis, 2002. 162(1): p. 55-61.

23. Sagar, S.M., D. Yance, and R.K. Wong, Natural health products that inhibit angiogenesis: a potential source for investigational new agents to treat cancer-Part 1. Curr Oncol, 2006. 13(1): p. 14-26.

24. Carmeliet, P. and R.K. Jain, Angiogenesis in cancer and other diseases. Nature, 2000. 407(6801): p. 249-57.

25. Weis, S.M. and D.A. Cheresh, Tumor angiogenesis: molecular pathways and therapeutic targets. Nat Med, 2011. 17(11): p. 1359-70.

26. Fong, T.A., et al., SU5416 is a potent and selective inhibitor of the vascular endothelial growth factor receptor (Flk-1/KDR) that inhibits tyrosine kinase catalysis, tumor vascularization, and growth of multiple tumor types. Cancer Res, 1999. 59(1): p. 99-106.

27. Ferrara, N., et al., Discovery and development of bevacizumab, an anti-VEGF antibody for treating cancer. Nat Rev Drug Discov, 2004. 3(5): p. 391-400.

28. Wilhelm, S.M., et al., Preclinical overview of sorafenib, a multikinase inhibitor

that targets both Raf and VEGF and PDGF receptor tyrosine kinase signaling. Mol Cancer Ther, 2008. 7(10): p. 3129-40.

29. Roberts, W.G., et al., Antiangiogenic and antitumor activity of a selective PDGFR tyrosine kinase inhibitor, CP-673,451. Cancer Res, 2005. 65(3): p. 957-66.

30. Ng, E.W., et al., Pegaptanib, a targeted anti-VEGF aptamer for ocular vascular disease. Nat Rev Drug Discov, 2006. 5(2): p. 123-32.

31. Joyce, G.F., Amplification, mutation and selection of catalytic RNA. Gene, 1989. 82(1): p. 83-7.

32. Ellington, A.D. and J.W. Szostak, In vitro selection of RNA molecules that bind specific ligands. Nature, 1990. 346(6287): p. 818-22.

33. Tuerk, C. and L. Gold, Systematic evolution of ligands by exponential enrichment: RNA ligands to bacteriophage T4 DNA polymerase. Science, 1990. 249(4968): p. 505-10.

34. Morris, K.N., et al., High affinity ligands from in vitro selection: complex targets. Proc Natl Acad Sci U S A, 1998. 95(6): p. 2902-7.

35. Ireson, C.R. and L.R. Kelland, Discovery and development of anticancer aptamers. Mol Cancer Ther, 2006. 5(12): p. 2957-62.

36. Jenison, R.D., et al., High-resolution molecular discrimination by RNA. Science, 1994. 263(5152): p. 1425-9.

37. Patel, D.J., et al., Structure, recognition and adaptive binding in RNA aptamer complexes. J Mol Biol, 1997. 272(5): p. 645-64.

38. Schmidt, K.S., et al., Application of locked nucleic acids to improve aptamer in vivo stability and targeting function. Nucleic Acids Res, 2004. 32(19): p. 5757-65.

39. Gold, L., et al., Aptamer-based multiplexed proteomic technology for biomarker discovery. PLoS One, 2010. 5(12): p. e15004.

40. Jayasena, S.D., Aptamers: an emerging class of molecules that rival antibodies in diagnostics. Clin Chem, 1999. 45(9): p. 1628-50.

41. Cho, M., et al., Quantitative selection of DNA aptamers through microfluidic selection and high-throughput sequencing. Proc Natl Acad Sci U S A, 2010. 107(35): p. 15373-8.

42. Nonaka, Y., K. Sode, and K. Ikebukuro, Screening and improvement of an anti-VEGF DNA aptamer. Molecules, 2010. 15(1): p. 215-25.

CHAPTER 2

APTAMER DISCOVERY USING YEAST DISPLAY CELL-SELEX

Summary

SELEX, the process of selecting aptamers, is often hampered by the difficulty of preparing target molecules in their native forms and by a lack of a simple yet quantitative assay for monitoring enrichment and affinity of reactive aptamers. In this study, I have applied the yeast surface display (YSD) system for cell-SELEX. First, I verified if the yeast surface display technique can successfully express our target proteins (PDGF-BB and VEGF) and serve as a platform of protein immobilization for aptamer binding. Afterwards, I performed a pilot yeast-cell-SELEX with known aptamers spiked-in ssDNA library. After nine rounds of selections, I successfully repeated the results from the previous published work and also selected new DNA aptamers for PDGF-BB.

The newly selected DNA aptamers for PDGF-BB have been quantitatively validated by flow cytometry with K_D=~30 nM and examined to specifically recognize PDGF-BB from structurally similar proteins.

Introduction and Significance

Aptamers are specific DNA or RNA oligonucleotides that have been isolated

from large random sequence pools for their ability to bind specific target molecules. Like antibodies, aptamers can bind with high affinity and specificity to target molecules ranging from proteins to small peptides [1, 2]. Moreover, aptamer have several advantages over antibodies, such as ease of handling, convenience of synthesis[3], breadth of potential targets, improved storage, and lack of immunogenicity. These features, in addition to their high affinity and specificity, have made them very promising in analytical, diagnostic[4], and therapeutic applications[5]. In fact, the first aptamer-based drug, called Pegaptanib (mucagen)[6, 7], is now available on the market. This indicates that aptamers can also be used directly as drugs.

Aptamers are obtained in vitro by a process called SELEX from a combinatorial library of DNA or RNA [8-10]. SELEX is an iterative procedure and often requires more than 10 successive cycles of selections and amplifications, where each SELEX cycle normally takes two days[11]. Each round of the selection comprises of several steps: 1) a random nucleic acid library containing 10^{13} ~10^{15} different sequences incubates with target proteins, 2) separating target-bound sequences from unbound ones, and 3) amplifying the selected ones for the next round. After successful selections of aptamers, aptamers are cloned and individually sequenced. In recent years, the conventional SELEX approach has been significantly improved in reducing laborious handlings in several different manners; however, the selection of aptamers to multiple targets in parallel is not well established. Also, the laborious purification of target proteins at the beginning stage and cloning to sequence individual aptamers at the last step remain to be tedious and time-consuming.

Selection of specific aptamers to intact cells, cell-SELEX, was first achieved in

1997[12]. In cell-SELEX, SELEX methodology is used with a complex mixture of cells as potential targets. Ligands to multiple targets are generated simultaneously during the selection process, and the binding affinities of these ligands for their targets are comparable to those found in similar experiments against pure targets. The approach was originally designed for when the clear marker target is unknown; so far, live cells of different cancers have been used in this process. As a result, certain numbers of aptamers have been generated from most cancer cell lines [13-16]. However, extended therapeutic application is hard to accomplish due to the lack of information for targeting proteins.

Yeast surface display (YSD) is a robust tool that has been employed successfully in isolating and engineering the affinity, specificity, and stability of antibodies[17-20], peptides[21], and proteins[22, 23]. YSD offers several advantages compared to other formats of display platforms such as phage display and the yeast-two hybrid method. Neither of these methods is effective for complex extracellular eukaryotic proteins, because of the absence of posttranslational modifications such as glycosylation and efficient disulfide isomerization. A protein of interest can be displayed on the surface of yeast by expression as a protein fusion to the Aga2p mating agglutinin protein. An extended advantage is that the quality control machinery of the yeast secretory pathway that routes mis-folded proteins into the degradation pathway ensures that proteins expressed on the surface are well folded. Furthermore, with YSD, displayed-protein expressions, soluble-ligand bindings, and ligand-binding kinetics can be examined and measured by flow cytometry. In the context of protein production, flow cytometry assay simultaneously gives analysis data which rules out the need to

separate steps of protein expression and protein functional analysis. As for the measurement of ligand-binding kinetics, the common measurement methods in quantification of equilibrium binding constants and dissociation rate are surface plasmon resonance (SPR), electrophoretic mobility shifted assay (EMSA), and fluorescence polarization(FP). These methods have good sensitivity, but more works and time are required. Compared to the binding examination by flow cytometry, these three methods not only require protein purification, but also protein immobilization, probe labeling.

Diagnostic procedures for cancer may include imaging, laboratory tests (including tests for tumor markers), tumor biopsy, endoscopic examination, surgery, or genetic testing. Imaging produces valuable pictures which can be used to detect tumors and other abnormalities, to determine the extent of disease, and to evaluate the effectiveness of treatment. Development of sensitive and specific molecular probe is still one of the main challenges in cancer imaging. In the context of molecular imaging, a variety of such probes have been developed [24-28]. Optical probes that yield high contrast target-to-background ratios are necessary to detect the micro-foci of cancer tumor. In general, aptamer probes have constant signals, while the image contrast is critically limited by a high background signals. Moreover, the cancer site can only be clearly observed after the physiological clearing of unbound aptamers, thus leading to a long diagnosis time, which further compromises the contrast by substantial consumption of bound aptamers. Therefore, ideal aptamer probes for in vivo cancer imaging should have high specificity targeting and high efficiency of clearance for the unbound probes.

Herein, I developed multiplexed-yeast-cell SELEX to select aptamers to many proteins in parallel. Taking advantage of next-generation-sequencing technology applied in this project, a thorough dataset from the sequencing result can be revealed to evaluate more candidates of aptamers. After aptamers are obtained, these aptamers will be adapted into target-activatable molecular probes of cancer imaging to enhance the contrast for in vivo diagnostic purpose. I expect these breakthroughs to accelerate current approaches of SELEX and facilitate molecular probes for cancer imaging.

Experimental Procedures

Procedure for yeast cell-SELEX

An initial library of 10^{15} DNA aptamers spiked with PDGF-BB Aptamer 1 (Pap1) [29] and VEGF165 Aptamer 7 (Vap7) [30] was screened against yeast cells expressing target proteins. Reactive aptamers against growth factors were dissociated from the cells by incubation with 10 mM dithiothreitol (DTT) for 10 min at 25℃, which would reduce disulfide bonds between two subunits of agglutinin, thereby releasing Aga2 and the bound aptamers from the cells. The mixture containing the aptamer complex was then cleaned up by a standard phenol-chloroform extraction and ethanol precipitation protocol [31], and amplified by PCR. The primer for the anti-sense strands to aptamers was phosphorylated at the 5' end and was digested by lambda exonuclease (NEB) for 30 minutes at 37℃ in 1X Lambda Exonuclease Reaction Buffer. To avoid chemical conjugation of aptamers with fluorescent dyes, I used phycoerythrin (PE)-conjugated streptavidin complexed with biotinylated

oligonucleotides (which I call 'capturing oligonucleotides') complementary to the constant region of the aptamers. After 4-10 rounds of SELEX, the aptamer pools were subject to high-throughput next-generation sequencing for bioinformatics analysis (see below).

Flow cytometry for detecting antigen expression and aptamer binding in yeast

Growth of yeast cells and induction of proteins was identical to the method described previously [21]. To verify the cell surface expression of target proteins, 5 µl of induced yeast culture was harvested, washed, and labelled at 30℃ for 30 min with anti-c-Myc antibody 9E10 (ATCC), anti-HA antibody 3F10 (Roche Applied Science), or anti-VEGF antibody (R&D) as primary antibodies in labelling buffer (PBS, 0.5% bovine serum albumin (BSA), 10 mM $MgCl_2$). After washing, cells were subsequently labelled at 4℃ for 10 min with goat anti-mouse IgG-PE (Santa Cruz) or rabbit anti-goat IgG-PE (Santa Cruz) secondary antibodies in labelling buffer. Cells were washed and re-suspended in 100 µl of labelling buffer and subjected to flow cytometry (Coulter Epics XL). To measure full-length aptamer binding to yeast, aptamers were first mixed with the biotinylated capturing oligonucleotides complementary to either 5' or 3' constant regions, heated at 95°C for 5 minutes, and then gradually cooled down to room temperature for 20 minutes. To measure the binding of truncated aptamers to yeast, truncated variants were synthesized with biotin attached at the 5' end. Aptamers with capturing oligonucleotides or biotinylated aptamers were then complexed with PE-conjugated streptavidin at a molar ratio of aptamer to streptavidin at 1:1. After washing, yeast cells were incubated with aptamer/streptavidin complex in

aptamer binding buffer (APBB; 10 mM HEPES, pH 7.9, 125 mM NaCl, 25 mM KCl, and 1 mM $MgCl_2$). After washing, cells were re-suspended in 100 μl of labelling buffer and subjected to flow cytometry. The Hill equation was fit to data (mean fluorescence intensities vs. concentration of aptamers) using Prism 5 (GraphPad) to determine the equilibrium dissociation constants.

High-throughput DNA Sequencing

The aptamer pools after SELEX rounds of 0, 4, 8, and 10 were chosen and subjected to a high-throughput DNA sequencing. A small portion of the PCR products from each selected pool listed above were PCR amplified using the primers that contain a unique 9-mer barcode and the adapters necessary for the HiSeq 2000 (Illumina) sequencing platform. High-throughput sequencing data derived from SELEX pools were filtered, clustered, and analyzed as previously described [32]. Processed sequences were analyzed separately for different pools, and those with >85% sequence identity were placed to the same clusters.

Results

To utilize YSD as a platform for immobilization of target proteins, proteins of interests are expressed at the yeast surface following a well-established protocol[19]. In short, a protein with either the N-terminal HA or the C-terminal c-myc epitope tag may be displayed on the surface of yeast by expression as a protein fusion to the Aga2p mating agglutinin protein. With the availability of the pNL6 plasmid, such

fusions can be expressed under the control of GAL1,10 galactose-inducible promoter. Aga1p is covalently attached to the cell wall via a phosphatidylinositol glycan tail, and Aga2p is disulfide bonded to Aga1p. The presence of the fusion protein on the cell surface may be detected of its ligand-binding activity by immunofluorescent labeling of epitope tags and examined by flow cytometry analysis.

Validate the feasibility of YSD as a novel platform of cell-SELEX.

To validate that YSD could be a new platform of cell-SELEX; a known DNA aptamer, Pap1 [29], screened from PDGF-BB protein has been synthesized and examined. Pap1 was being isolated from an 80-bp synthetic ssDNA library whose composition is a 40-bp variable region flanked by two 20-bp constant regions at both sides. The PDGF-BB protein has been expressed to the yeast surface and examined the function through YSD system and immunofluorescent labeling of c-myc tag by flow cytometry assay. In order to quantitatively and efficiently detect the florescent signal from the binding of aptamer to yeast cells by flow cytometry, the novel notion of 20-bp biotinylated capturing oligo (B-CO) has been designed (Figure 2-1b). The design of B-CO is composed by a 20-mer oligo with 5'-biotin labeled, and the sequences of the 20-mer oligo are complementary to the forward side of the constant regions on the aptamers. By taking the advantage of tetrameric streptavidin's high affinity for biotin with a dissociation constant (K_d) on the order of $\approx 10^{-14}$ mol/L, the ratio adjustment for aptamer_B-CO hybrid coupled to strepavidin could be applied for various aptamers with different intensity of binding affinities. Through this approach, the strongest signal of florescent intensity can be observed by flow cytometry. The avidity

introduced by using the coupled streptavidin and B-CO_aptamer can increase the binding affinity of aptamers and stabilized the tetramerized structure. After annealing the B-CO to Pap1 during the aptamer refolding process, the Pap1_B-CO hybrid is ready to bind to the streptavidin that has been fluorescently labeled. At the same time, to estimate the dissociation constant (K_D) of aptamers to antigens by flow cytometry, florescent intensities generated by serial diluted aptamer are collected to calculate the dissociation constant (Figure 2-1a). The preliminary result (Figure 2-1c) indicates that:

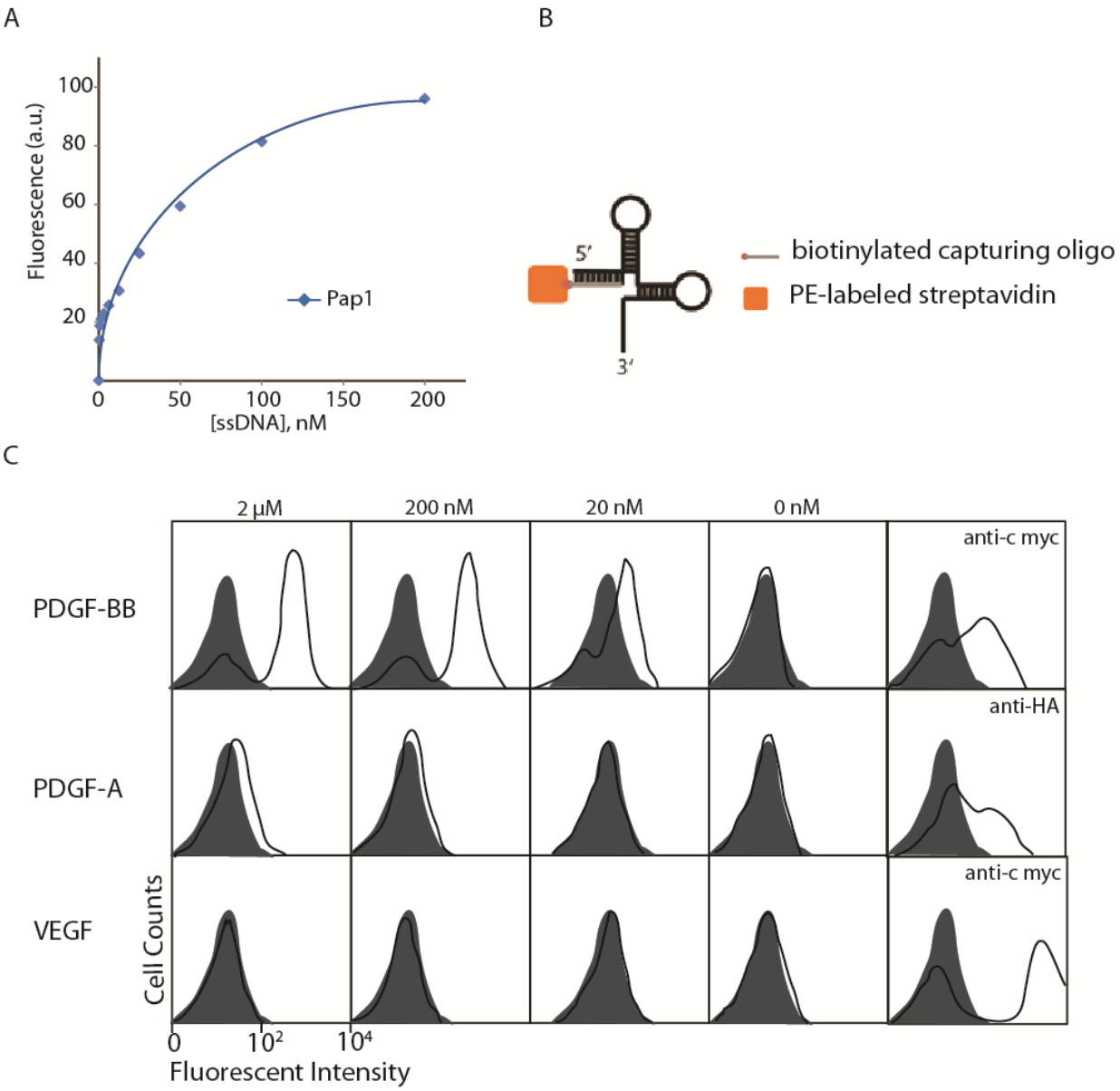

Figure2-1. Verification of cell-SELEX with yeast surface display system. (a) Dissociation constant (Kd) measurement from flow cytometry. The binding affinity of Pap1 measured by flow cytometry assay is 27.3 nM. The formula that calculated Kd equals to $[ssDNA]_{1/2\ Fluorescence(Max)}$. (b) The design of biotinylated capturing oligo coupling to streptavidin-PE. (c) Binding of Pap1 and anti-c-myc/ anti-HA antibody to yeast before (shaded) and after (solid line) target protein expressed on the surface.

1) Pap1 shows concentration-dependent binding to yeast-surface expressed PDGF-BB.
2) Compared to the panel of antigen PDGF-AA and PDGF-BB, YSD system is an exquisite platform to express homologous proteins where specific aptamers can differentiate their target protein.
3) Compared to the panel of antigen PDGF-BB and VEGF, YSD system is also a facile platform to express proteins that are structurally similar. I can examine the binding specificity of aptamer to its target protein in this way.
4) To make the best use of flow cytometry results, a semi-quantitative way have been devised to rapidly estimate the affinity of an aptamers. After analysis, the dissociation constant of an aptamer can be calculated from collecting the data of serial-diluted samples by flow cytometry.

Establish a novel platform for multiplexed-yeast-cell SELEX by using YSD to isolate specific aptamers.

To conduct a pilot yeast-cell-SELEX with known aptamers, a spiked-in library that contains Pap1, VEGF165 Aptamer 7 (Vap7) [30]and random library in the molar ratio of $1:1:10^6$ with the complexity ~10^{14} has been made. The ssDNA library contains 40 bp-variable region in the middle flanked by 20 bp-constant regions at both sides which also serve as primer binding sequences for PCR. (Library design: 5'-TCCCACGCATTCTCCACATC-[40N]-CCTTTCTGTCCTTCCGTCAC-3').

The aptamer binding buffer (APBB, 10mM HEPES (pH=7.9), 125 mM NaCl, 25 mM KCl, and 1 mM $MgCl_2$) used throughout the whole selection to dissolve the

ssDNA library, perform the incubation of ssDNA library to yeast, and washing is the same. The flow of the pilot yeast-cell-SELEX is described shortly as followed (Figure 2-2a). Before being incubated with target protein expressed yeast, the ssDNA library is heat-denatured at 95^{o}C to form the secondary structure while the temperature gradually cools down. The secondary structure is critical for binding to target. Negative selection, the selection of ssDNA libraries with non-specific protein expressed yeast, is always performed at the initial step of every round of selection to get rid of non-specific binders, and is followed up by target-protein selection. After the incubation of library with target protein expressed yeast, appropriate washes are applied to get rid of the unbound ssDNA and heat-elution is performed to retrieve the bound ssDNA. The eluted ssDNA are then amplified by PCR for the subsequent round of selection and high-through-put sequencing. To amplify the retrieved ssDNA, forward and reverse primers are designed to prime the constant region for PCR reaction. The reverse primer is 5'-phosphorylated to generate the phosphorylated reverse strand. Lambda exonuclease is a highly processive 5' to 3′ exodeoxyribonuclease that selectively digests the 5′-phosphorylated strand of dsDNA. For this purpose, a 5′-phosphate group is introduced into one strand of dsDNA by performing PCR where only one of the two primers is 5′-phoshorylated. The phosphorylated strand is then removed by digestion with lambda exonuclease. The progress of selection and enrichment are monitored by flow cytometry.

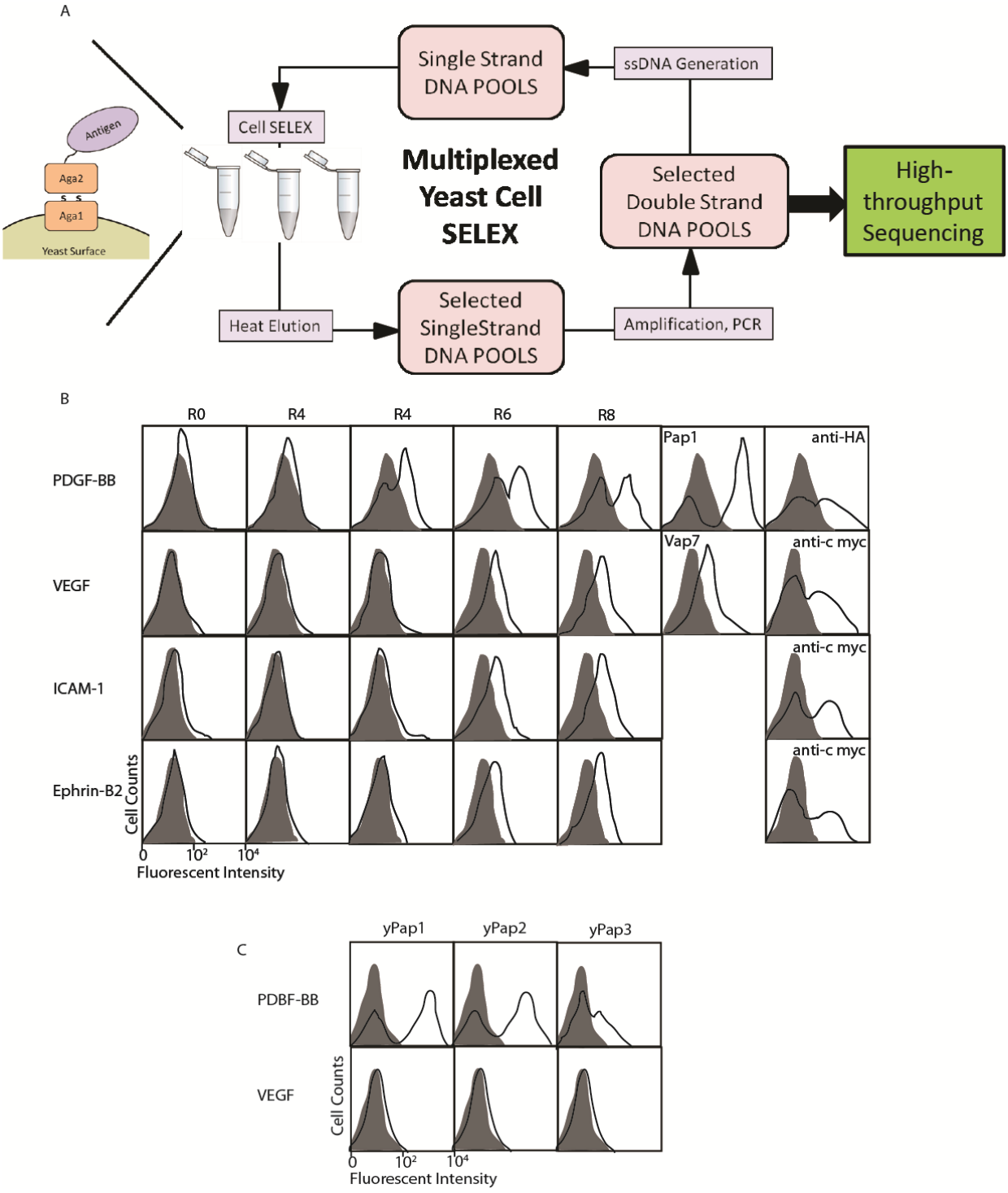
A
Single Strand DNA POOLS
ssDNA Generation
Cell SELEX
Antigen
Aga2
Aga1
Yeast Surface
Multiplexed Yeast Cell SELEX
Selected Double Strand DNA POOLS
High-throughput Sequencing
Heat Elution
Selected SingleStrand DNA POOLS
Amplification, PCR
B
R0
R4
R4
R6
R8
Pap1
anti-HA
PDGF-BB
Vap7
anti-c myc
VEGF
anti-c myc
ICAM-1
anti-c myc
Ephrin-B2
Cell Counts
0
10²
10⁴
Fluorescent Intensity
C
yPap1
yPap2
yPap3
PDBF-BB
VEGF
Cell Counts
0
10²
10⁴
Fluorescent Intensity

Figure 2-2. Characterization of Multiplexed-Yeast Cell SELEX. (a). Schematic flow of DNA aptamer selection using the yeast-cell SELEX. (b). Monitoring the progress of yeast-cell SELEX from R0 to R8. The histograms are showing detections of target screened libraries, known aptamers, and anti-c-myc antibody to yeast before (shaded) and after (thick lines) target protein expressed on the surface. (c). Binding test of newly selected aptamers of PDGF-BB to yeast before (shaded) and after (thick lines) target protein expressed on the surface.

In this experimental design, spike-in library is applied to PDGF-BB and VEGF165, and random library is performed in parallel with intercellular adhesion molecule 1 (ICAM-1) and ephrin B2 to validate yeast-cell-SELEX. Based on the result of progress of selection by flow cytometry assay (Figure 2-2b), PCR products from round4, round5, round7, and round9 are sequenced by performing high-throughput DNA sequencing technology with the Genome Analyzer II (Illumina).

After the sequencing, the collected results are clustered and analyzed (Table 1); some of the top-ranked candidates are synthesized and tested for binding. The preliminary result indicates that:

1) The top sequences from the PDGF-BB pool (Table 1) and VEGF165 pool (data not shown) are the spiked-in aptamers; this finding is revealed that spiked-aptamer can be enriched and fished through yeast-cell-SELEX.
2) In addition to the spiked-in aptamers, some of the other aptamers also got enriched and isolated at later rounds of SELEX in the PDGF-BB pool. These aptamers (yPap1, yPap2, and yPap3) also showed binding of high affinity and specificity compared to the spiked-in Pap1 (Figure 2-2c).
3) Interestingly, besides the spiked-in aptamer, these top-two-enriched aptamer (yPap1, yPap2) are identical or with high similarities to the top-two aptamers that have been previously published [29].
4) The possible explanation for the failure of the rest of the three antigens could be that the yeast cell surface is negatively charged which contributes the repelling force to ssDNA that is also negatively charged. The likelihood of getting high-affinity aptamers is thought to be related to the target protein's isoelectric point

(pI). There is an inverse correlation between protein charge and aptamer K_d [33]. When a basic protein which usually has a high pI being incubated in APBB at pH=7.9, the protein net charge is reduced which considerably increases the affinity to be bound with ssDNA.

5) Another possible explanation for the failure of the rest of the three antigens could be that the variety of the current ssDNA library is not complex enough. The ssDNA-library with longer variable region could be ideal to increase the complexity of the ssDNA library.

Table 2-1. Enriched aptamer sequences selected against PDGF-BB.

Name in the thesis	Aptamer ID	Sequences of selected aptamers (5'-->3')	Reads of Each Cluster			
			R4	R5	R7	R9
yPap1	1	GATACTGAGCATCGTACATGATCCCGCAACGGGCAGTATT	3238	17430	49785	37270
Pap1	2	ATAAGCTGAGCATCTTAGATCCCCGTCAAGGGCAGCGTAA	26605	22216	39303	30837
yPap2	3	AGTTGAATGGTGTGGTCACTTCCAGTCCCGCAGGGCACAC	93	590	17679	2340
yPap3	4	GATACTGAGCATCGTACATGATCCCGTCAAGGGCAGCGTAA	38	105	536	480
	5	TGAGCATCTTAGATCCCGTCAAGGGCAGCGTAA	375	368	453	458
	6	ATAAGCTGAGCATCTTAGATCCCGCAACGGGCAGTATT	13	85	645	365
	7	ATAAGCTGAGCATCTTAGATCCCCGTCAAGGGGCAGCTA	98	110	759	219
	8	ATAAGCTGAGCATCTTTAGATCCCTCAAGGGCAGCGTAA	82	112	207	148
	9	AGTTGGTGTGGTCACTTCCAGTCCCGCAGGGCACAC	0	11	2507	142
	10	AAGCTGAGCATCTTAGATCCCTGTCAGGGCAGCGTAA	72	110	216	142
	11	GATACTGAGCATCTTAGATCCCCCAAGGGCAGCGTAA	25	29	170	135
	12	ATAAGCGGAGCATCTTAGATCCCCGTCAGGGGCAGGGTAA	59	91	312	123
	13	ACGAAGGTGGTTGCCCATGTCCTGCTAAGGGAATGTAAGT	0	9	2075	119
	14	AAAAGCTGAGCATCTTAGATCCCCGTCATGGGCAGCGTAA	161	82	229	117
	15	AACTGGGCATGGTACGATCATGTTAAGCCGGCTTCCCAGT	0	2	1483	72
	16	CCATAAGCTGAGCATCTTAGATCCCCGTCAGGGGCAGCCTAA	10	34	109	55
	17	ATAAGCTGAGCATCTTAGATCCCTGTCAAGGGGTAGCGAA	20	60	78	53
	18	GCACTCTGGGGGTGGACGGGCCGGGT	192	61	16	49
	19	ACATCGATACTGAGCATCGTACATGATCCCGCAACGGGCAGTA	4	17	50	43
	20	ATAAGCTGAGCATCTTAGATCCCCGTCAAGGCCAGTGCAA	123	49	65	42

Discussion

Here I demonstrate that our novel system, YSD-SELEX, is highly efficient in the discovery of high-affinity DNA aptamer binder. First of all, I established a new yeast-cell-based assay for aptamer binding testing. I expressed PDGF-BB proteins to the surface of the yeast cells and synthesized the known DNA aptamers against PDGF-BB[29]. To confirm the protein expression to the yeast surface, I tested the binding of either the HA tag or c-myc tag that are fusions to the protein of interest with antibodies and performed flow cytometry to evaluate the protein expression to the protein of interest. To fluorescently label the DNA aptamers, I designed a short DNA sequences, B-CO, that's complementary to the forward side of the constant region from the DNA aptamer with a biotin labeled at its 5'-end, and mix with the DNA aptamer to 1:1 molar ratio during the aptamer refolding process to form the duplex. After the mixture of DNA aptamers and B-CO is generated, I applied the pre-formed complex with the same molar ratio of streptavidin-PE to fluorescently label the DNA aptamer for flow cytometry. By performing the binding test of using known DNA aptamer of PDGF-BB, I validated the YSD system can serve as a protein immobilization platform on yeast cells as a semi-quantitative way to rapidly estimate the affinity of an aptamers.

To further utilize the YSD system for creating new aptamers, I conducted a pilot yeast-cell-SELEX with known aptamers, a spiked-in library that contains Pap1, Vap7[30] and random library in the molar ratio of $1:1:10^6$ with the complexity ~10^{14}

has been made. The ssDNA library contains a 40 bp-variable region in the middle flanked by 20 bp-constant regions at both sides which also serve as primer binding sequences for PCR. (Library design: 5'-TCCCACGCATTCTCCACATC-[40N]-CCTTTCTGTCCTTCCGTCAC-3'). I also developed the multiplexed-yeast-cell SELEX for aptamer selections by using the YSD system for PDGF-BB, VEGF-A, ICAM-I, and Ephrin-B2 in parallel. Taking advantage of next-generation-sequencing technology applied in this project, a thorough dataset from the sequencing result can be revealed to evaluate more candidates of aptamers (Table 2-1).

The high similarity of the PDGF-BB aptamers selected from YSD-SELEX and microfluidic SELEX (M-SELEX) M-SELEX gives us a lot of room to tackle the reasons lead to the results. First of all, the starting materials of SELEX, the ssDNA library, could be the possible resource of creating identical aptamers from two different methods of aptamer selections. Both Cho *et. al.* [29] and our group ordered the ssDNA library with same length of variable region (40 nucleotides), and purchased from the same vendor (Integrated DNA Technologies). The theoretical complexity of the library (10^{24}) is more comprehensive than the actual complexity for the experimental library (10^{15}), and it's nearly impossible for a pipeline to generate two identical ssDNA libraries. However, I am not sure how the synthesis platforms from Integrated DNA Technologies had been automated and programmed that may generate two identical ssDNA libraries for the same length at two different time periods or if the vendor saved some aliquots from the original order of the Cho *et. al.* [29] and gave us an aliquot to complete our order. Secondly, the Craighead group from the aptamer community at Cornell University have experienced and proved selections that are done

with the same RNA library with the same sequences but with two different methods (traditional SELEX and RAPID-SELEX) could possibly enrich identical binders for the same target proteins (data not yet publish).

The Yeast Surface Display system has been validated and established for a powerful and efficient platform for aptamer selections. YSD-SELEX will be the main focus for the following application derived from the validation in this chapter. After aptamers are obtained and well-characterized, these aptamers will be adapted into target-activatable molecular probes of cancer imaging to enhance the contrast for in vivo diagnostic purpose. I expect these breakthroughs to accelerate current approaches of SELEX and facilitate molecular probes for cancer imaging.

REFERENCES

1. Jenison, R.D., et al., High-resolution molecular discrimination by RNA. Science, 1994. 263(5152): p. 1425-9.
2. Patel, D.J., et al., Structure, recognition and adaptive binding in RNA aptamer complexes. J Mol Biol, 1997. 272(5): p. 645-64.
3. Jayasena, S.D., Aptamers: an emerging class of molecules that rival antibodies in diagnostics. Clin Chem, 1999. 45(9): p. 1628-50.
4. Kwon, J.A., et al., High diagnostic accuracy of antigen microarray for sensitive detection of hepatitis C virus infection. Clin Chem, 2008. 54(2): p. 424-8.
5. Tang, Z., et al., Selection of aptamers for molecular recognition and characterization of cancer cells. Anal Chem, 2007. 79(13): p. 4900-7.
6. Rakic, J.M., P. Blaise, and J.M. Foidart, Pegaptanib and age-related macular degeneration. N Engl J Med, 2005. 352(16): p. 1720-1; author reply 1720-1.
7. Ng, E.W., et al., Pegaptanib, a targeted anti-VEGF aptamer for ocular vascular disease. Nat Rev Drug Discov, 2006. 5(2): p. 123-32.
8. Ellington, A.D. and J.W. Szostak, In vitro selection of RNA molecules that bind specific ligands. Nature, 1990. 346(6287): p. 818-22.
9. Robertson, D.L. and G.F. Joyce, Selection in vitro of an RNA enzyme that specifically cleaves single-stranded DNA. Nature, 1990. 344(6265): p. 467-8.
10. Tuerk, C. and L. Gold, Systematic evolution of ligands by exponential enrichment: RNA ligands to bacteriophage T4 DNA polymerase. Science, 1990. 249(4968): p. 505-10.

11. Park, S.M., et al., A method for nanofluidic device prototyping using elastomeric collapse. Proc Natl Acad Sci U S A, 2009. 106(37): p. 15549-54.
12. Morris, K.N., et al., High affinity ligands from in vitro selection: complex targets. Proc Natl Acad Sci U S A, 1998. 95(6): p. 2902-7.
13. Blank, M., et al., Systematic evolution of a DNA aptamer binding to rat brain tumor microvessels. selective targeting of endothelial regulatory protein pigpen. J Biol Chem, 2001. 276(19): p. 16464-8.
14. Cerchia, L., et al., Neutralizing aptamers from whole-cell SELEX inhibit the RET receptor tyrosine kinase. PLoS Biol, 2005. 3(4): p. e123.
15. Shangguan, D., et al., Aptamers evolved from live cells as effective molecular probes for cancer study. Proc Natl Acad Sci U S A, 2006. 103(32): p. 11838-43.
16. Sefah, K., et al., Molecular recognition of acute myeloid leukemia using aptamers. Leukemia, 2009. 23(2): p. 235-44.
17. Kieke, M.C., et al., Isolation of anti-T cell receptor scFv mutants by yeast surface display. Protein Eng, 1997. 10(11): p. 1303-10.
18. Boder, E.T., K.S. Midelfort, and K.D. Wittrup, Directed evolution of antibody fragments with monovalent femtomolar antigen-binding affinity. Proc Natl Acad Sci U S A, 2000. 97(20): p. 10701-5.
19. Chao, G., et al., Isolating and engineering human antibodies using yeast surface display. Nat Protoc, 2006. 1(2): p. 755-68.
20. Hu, X., et al., Combinatorial libraries against libraries for selecting neoepitope activation-specific antibodies. Proc Natl Acad Sci U S A, 2010. 107(14): p.

6252-7.

21. Boder, E.T. and K.D. Wittrup, Yeast surface display for screening combinatorial polypeptide libraries. Nat Biotechnol, 1997. 15(6): p. 553-7.
22. Kieke, M.C., et al., Selection of functional T cell receptor mutants from a yeast surface-display library. Proc Natl Acad Sci U S A, 1999. 96(10): p. 5651-6.
23. Kieke, M.C., et al., High affinity T cell receptors from yeast display libraries block T cell activation by superantigens. J Mol Biol, 2001. 307(5): p. 1305-15.
24. Weissleder, R., et al., In vivo imaging of tumors with protease-activated near-infrared fluorescent probes. Nat Biotechnol, 1999. 17(4): p. 375-8.
25. Jiang, T., et al., Tumor imaging by means of proteolytic activation of cell-penetrating peptides. Proc Natl Acad Sci U S A, 2004. 101(51): p. 17867-72.
26. Blum, G., et al., Noninvasive optical imaging of cysteine protease activity using fluorescently quenched activity-based probes. Nat Chem Biol, 2007. 3(10): p. 668-77.
27. Hama, Y., et al., A target cell-specific activatable fluorescence probe for in vivo molecular imaging of cancer based on a self-quenched avidin-rhodamine conjugate. Cancer Res, 2007. 67(6): p. 2791-9.
28. Shi, H., et al., Activatable aptamer probe for contrast-enhanced in vivo cancer imaging based on cell membrane protein-triggered conformation alteration. Proc Natl Acad Sci U S A, 2011. 108(10): p. 3900-5.
29. Cho, M., et al., Quantitative selection of DNA aptamers through microfluidic selection and high-throughput sequencing. Proc Natl Acad Sci U S A, 2010. 107(35): p. 15373-8.

30. Nonaka, Y., K. Sode, and K. Ikebukuro, Screening and improvement of an anti-VEGF DNA aptamer. Molecules, 2010. 15(1): p. 215-25.

31. Chomczynski, P. and N. Sacchi, Single-step method of RNA isolation by acid guanidinium thiocyanate-phenol-chloroform extraction. Anal Biochem, 1987. 162(1): p. 156-9.

32. Latulippe, D.R., et al., Multiplexed microcolumn-based process for efficient selection of RNA aptamers. Anal Chem, 2013.

33. Ahmad, K.M., et al., Probing the limits of aptamer affinity with a microfluidic SELEX platform. PLoS One, 2011. 6(11): p. e27051.

CHAPTER 3

DISCOVERING APTAMERS BY CELL-SELEX AGAINST HUMAN SOLUBLE GROWTH FACTORS ECTOPICALLY EXPRESSED ON YEAST CELL SURFACE

Summary

[3]SELEX, the process of selecting aptamers, is often hampered by the difficulty of preparing target molecules in their native forms and by a lack of a simple yet quantitative assay for monitoring enrichment and affinity of reactive aptamers. In this study, I sought to discover DNA aptamers against human serum markers for potential therapeutic and diagnostic applications. To circumvent soluble expression and immobilization for performing SELEX, I ectopically expressed soluble growth factors on the surface of yeast cells to enable cell-SELEX and devised a flow cytometry-based method to quantitatively monitor progressive enrichment of specific aptamers. High-throughput sequencing of selected pools revealed that the emergence of highly enriched sequences concurred with the increase in the percentage of reactive aptamers shown by flow cytometry. Particularly, selected DNA aptamers against VEGF were specific and of high affinity (K_D = ~ 1 nM), and demonstrated a potent inhibition of

[3] This chapter is modified with the permission of the publisher from Meng H, Pagano J, White B, Toyoda Y, Min I, Craighead H, Shalloway D, Lis J, and Jin M. Discovering aptamers by Cell-SELEX against human soluble growth factors ectopically expressed on yeast cell surface. (Submitted to PLOS ONE.) Hsien-Wei Meng designed the study, conducted the experiments, analyzed the data and wrote the paper.

capillary tube formation of endothelial cells, comparable to the effect of a clinically approved anti-VEGF antibody drug, bevacizumab. Considering the fact that many mammalian secretory proteins have been functionally expressed in yeast, the strategy of implementing cell-SELEX and quantitative binding assay can be extended to discover aptamers against a broad array of soluble antigens.

Introduction and Significance

Aptamers are specific DNA or RNA oligonucleotides selected from large random sequence pools for their ability to bind specific target molecules. Like antibodies, aptamers can bind with high affinity and specificity to targets ranging from proteins to small molecules [1-3]. Aptamers are obtained in vitro by a process called SELEX (Systematic Evolution of Ligands by EXponential enrichment [4-6] consisting of repeated rounds of negative selection and enrichment of nucleic acid binders against the molecules immobilized on membranes or beads. Selection of specific aptamers against cell surface proteins has also been performed using intact cells, a method termed cell-SELEX[7]. This method is particularly advantageous if the target molecules are cell surface or trans-membrane molecules not amenable to soluble expression and purification, and is necessary if aptamers are selected directly against surface markers specific to certain cell types.

Growth factors, cytokines, and other soluble molecules present in the blood are important signalling molecules, mediating various functions in normal physiology [8] and are also implicated in the onset and progression of many diseases[9]. Antibodies

against serum proteins have been approved or are under investigation as therapeutic agents for various pathological conditions including cancer and inflammatory diseases [10-12]. More recently, aptamers as binding reagent have been developed against serum proteins with comparable affinity and specificity as antibodies [13]. To circumvent a difficulty with preparing antigens in solution to be used for selection of binding reagents, I have previously shown that mammalian cell surface molecules ectopically expressed on the surface of yeast cells provided a highly efficient platform for selection of specific, high-affinity antibodies [14]. Rapid discovery of specific antibodies was attributed to the fact that the molecules expressed in yeast cells as a fusion to a cell wall protein, agglutinin, are natively folded, and expressed at high density on cell surface. In addition, the complexity of other naturally expressed cell surface molecules would serve as competitive decoys for rapid depletion of non-specific binders. Here I extend these strategies for antibody selection to the discovery of aptamers against human serum growth factors that are ectopically displayed on the surface of yeast cells using a standard cell-SELEX procedure.

Among the soluble growth factors in serum, I have chosen VEGF, PDGF-A, and IL-6 as target antigens for selection of aptamers. VEGF and PDGF are the essential soluble factors for promoting vasculature growth, and antagonists of the family of growth factors or their receptors have been developed as drugs to treat several types of cancers[15]. Currently available VEGF antagonists exist at least in three different forms: as a monoclonal antibody (i.e., bevacizumab), as an RNA aptamer (i.e., pegaptanib[16]), and as a fusion of VEGF receptor (VEGFR) and the antibody Fc domain (i.e., VEGF-Trap [17]). Currently, pegaptanib is the only FDA-approved

aptamer drug and is being used for treating age-related macular degeneration [18]. By ectopically expressing soluble proteins as cell surface molecules in yeast, I were able to use the cell-SELEX strategy to isolate specific DNA aptamers against VEGF and PDGF-A. Using high-throughput sequencing of selected pools generated during SELEX rounds, I isolated DNA aptamers against VEGF having higher binding affinity to VEGF in physiological buffer than previously reported DNA aptamers. By truncating full-length VEGF aptamers into shorter fragments containing all or a part of conserved structural motifs, I identified a minimal key structural motif for these aptamers. Various truncated aptamers against VEGF effectively blocked the capillary tube formation of endothelial cells, an assay used to gauge antagonist potency for blocking angiogenesis, comparable to the effect of the monoclonal antibody, bevacizumab.

The procedure developed in this study can readily be adapted for the discovery of high affinity aptamers against a much larger set of targets by circumventing the challenge of functional expression, purification, and immobilization of mammalian soluble proteins. At the same time, flow cytometry-based assay for quantitative measurement of binding affinity and enrichment of reactive aptamers will aid rapid screening of highly enriched sequences revealed by high-throughput sequencing**.**

Experimental Procedures

Procedure for yeast cell-SELEX.

An initial library of 10^{15} DNA aptamers was screened against yeast cells

expressing target proteins. Reactive aptamers against growth factors were dissociated from the cells by incubation with 10 mM DTT for 10 min at 25℃, which would reduce disulfide bonds between two subunits of agglutinin, thereby releasing Aga2 and the bound aptamers from the cells. The mixture containing the aptamer complex was then cleaned up by a standard phenol-chloroform extraction and ethanol precipitation protocol [19], and amplified by PCR. The primer for the anti-sense strands to aptamers was phosphorylated at the 5' end and was digested by lambda exonuclease (NEB) for 30 minutes at 37℃ in 1X Lambda Exonuclease Reaction Buffer. To avoid chemical conjugation of aptamers with fluorescent dyes, I used phycoerythrin (PE)-conjugated streptavidin complexed with biotinylated oligonucleotides (which I call 'capturing oligonucleotides') complementary to the constant region of the aptamers. After 4-10 rounds of SELEX, the aptamer pools were subject to high-throughput next-generation sequencing for bioinformatics analysis (see below).

Flow cytometry for detecting antigen expression and aptamer binding in yeast.

Growth of yeast cells and induction of proteins was identical to the method described previously [20]. To verify the cell surface expression of target proteins, 5 μl of induced yeast culture was harvested, washed, and labelled at 30℃ for 30 min with anti-c-Myc antibody 9E10 (ATCC), anti-HA antibody 3F10 (Roche Applied Science), or anti-VEGF antibody (R&D) as primary antibodies in labelling buffer (PBS, 0.5% bovine serum albumin (BSA), 10 mM $MgCl_2$). After washing, cells were subsequently labelled at 4℃ for 10 min with goat anti-mouse IgG-PE (Santa Cruz) or rabbit anti-

goat IgG-PE (Santa Cruz) secondary antibodies in labelling buffer. Cells were washed with labelling buffer and re-suspended in 100 µl of labelling buffer and subjected to flow cytometry (Coulter Epics XL). To measure full-length aptamer binding to yeast, aptamers were first mixed with the B-CO complementary to either 5' or 3' constant regions, heated at 95℃ for 5 minutes, and then gradually cooled down to room temperature for 20 minutes to form the duplex with B-CO at the forward site of constant region and the secondary structure of the aptamers. To measure the binding of truncated aptamers to yeast, truncated variants were synthesized with biotin attached at the 5' end. Aptamers with capturing oligonucleotides or biotinylated aptamers were then complexed with PE-conjugated streptavidin at a molar ratio of aptamer to streptavidin at 1:1. After washing, yeast cells were incubated with aptamer/streptavidin complex in aptamer binding buffer (APBB; 10 mM HEPES, pH 7.9, 125 mM NaCl, 25 mM KCl, and 1 mM $MgCl_2$). After washing, cells were re-suspended in 100 µl of labelling buffer and subjected to flow cytometry. The Hill equation was fit to data (mean fluorescence intensities vs. concentration of aptamers) using Prism 5 (GraphPad) to determine the equilibrium dissociation constants.

Flow cytometry for measuring VEGF binding to HeLa cells.

HeLa cells with the expression of VEGFR were used to measure the inhibition of VEGF binding to VEGFR by selected aptamers. Serially diluted VEGF (Syd Labs) was pre-incubated with the full-length hVap2 for 30 min at 4℃, and the mixture was then applied to HeLa. VEGF binding to HeLa was detected by anti-VEGF polyclonal antibodies (R&D) followed by a rabbit anti-goat IgG-PE-conjugated secondary

antibody (Santa Cruz).

High-throughput DNA Sequencing.

The aptamer pools after SELEX rounds of 0, 4, 8, and 10 were chosen and subjected to a high-throughput DNA sequencing. A small portion of the PCR products from each selected pool listed above were PCR amplified using the primers that contain a unique 9-mer barcode and the adapters necessary for the HiSeq 2000 (Illumina) sequencing platform. High-throughput sequencing data derived from SELEX pools were filtered, clustered, and analyzed as previously described [21]. Processed sequences were analyzed separately for different selected pools, and those with >85% sequence identity were placed to the same clusters.

Gel-shift assay with fluorescein-labeled aptamer.

Aptamers were phosphorylated at the 5' end with adenosine 5'-[γ-thio] triphosphate (Sigma-Aldrich), which were subsequently labelled with 5-Iodoacetamidofluorescein (5-IAF) (Sigma-Aldrich), following a protocol previously described [22]. VEGF and DNA were mixed and incubated in binding buffer (10 mM HEPES, pH 7.9, 125 mM NaCl, 25 mM KCl, and 1 mM $MgCl_2$) at room temperature for 2 hours, and were analyzed on a 5% polyacrylamide gel, run at 120 V in 1X tris/borate/EDTA (TBE) buffer at 4℃ for 1-1.5 hours. The gel was then imaged by a phosphor-imager (Typhoon 9400 imager, GE Healthcare Life Sciences). The intensity of the bands were quantified by ImageJ (http://rsbweb.nih.gov/ij/, NIH), and the Hill equation was fit to data points to determine the equilibrium dissociation constant by

using Prism 5 (GraphPad).

Human umbilical vein endothelial cell (HUVEC) capillary tube formation assay.

Capillary tube formation assay was performed with a growth factor reduced Matrigel (BD Biosciences). After thawing overnight at 4°C, 50 μL Matrigel was placed into each well of a pre-chilled 96-well plate (Millipore), and the Matrigel was allowed to polymerize for 30 minutes in the 37°C incubator. HUVECs (Lonza) were placed in the wells coated with Matrigel at 2,000 cells per well in EGM-2 (EGM-2 BulletKit; Lonza) containing 5% FBS. Cells were treated with antibodies (bevacizumab or isotope control) or aptamers used at 16.6 μM. After 6-12 hours of incubation, three randomly captured microscopic (Observer.Z1, Zeiss) images were recorded. Tube length was quantified by Angiogenesis Analyzer for ImageJ software (http://rsbweb.nih.gov/ij/, NIH). Tube length was assessed by drawing a line along each tube and measuring the length of the line in pixels. The average of three fields was taken as the mean value for each treatment.

Results

Cell-SELEX implemented by ectopic expression of human growth factors on yeast cell surface.

DNA aptamers of 100 nucleotides (nt) in length were designed to contain a 60-nt variable region flanked by 20-nt constant regions, which serve as the primer annealing sites for PCR. The growth factors (PDGF-A, PDGF-B, VEGF, and IL-6) were

expressed as fusions to the cell wall protein agglutinin for cell surface presentation to enable cell-SELEX procedure (Figure 3-1a). A single round of SELEX consisted of negative selection of aptamers with yeast cells expressing unrelated proteins (PDGF-B or epidermal growth factor receptor), positive selection of specific aptamers that bind to target antigens, and PCR amplification. Double-stranded PCR products, composed of a 5'-OH sense strand and a 5'-phosphate anti-sense strand, were treated with lambda exonuclease to digest anti-sense strands and recover single-stranded aptamers [23]. The enrichment of aptamers specific to target antigens was confirmed by an increase in the percentage of binders measured by flow cytometry. In order to avoid direct labelling or chemical modification of aptamers for attaching fluorescent dyes, biotinylated oligonucleotides complementary to either 5' or 3' constant regions were used to form a complex with aptamers, which were then added to PE-conjugated streptavidin (Figure 3-1b). After eight to ten rounds of SELEX, a substantial (24-76%) sub-population of aptamers exhibited binding to PDGF-A and VEGF antigens (Figure 3-1c). Considering the diversity of the initial library (10^{15}), the enrichment factor for our cell-SELEX was estimated to be 100-fold per cycle. The percentage of reactive aptamers against IL-6 was lower, reaching ~12% at the final round.

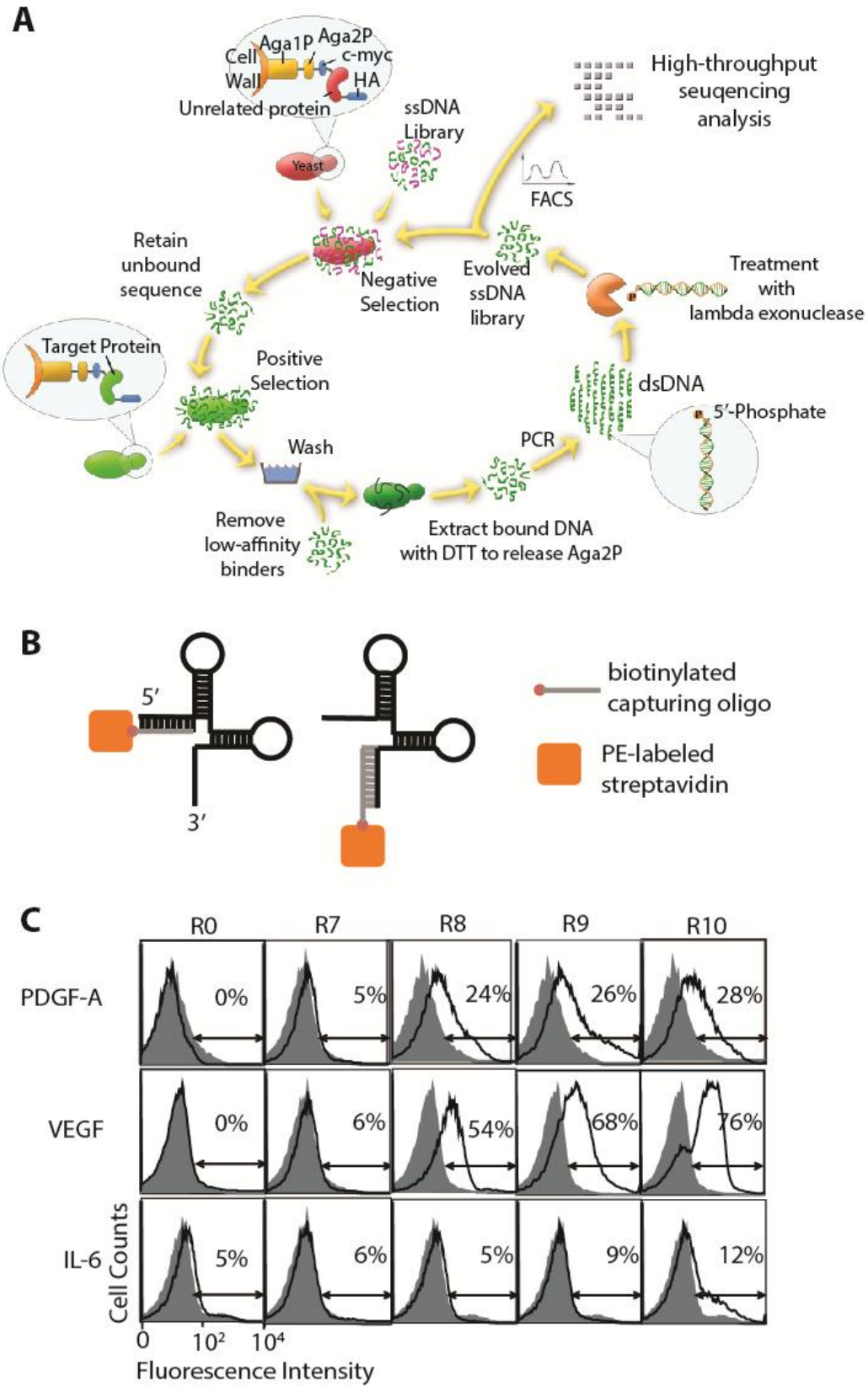
A
Aga1P
Aga2P
Cell Wall
c-myc
HA
Unrelated protein
Yeast
ssDNA Library
High-throughput seuqencing analysis
FACS
Retain unbound sequence
Negative Selection
Evolved ssDNA library
Treatment with lambda exonuclease
Target Protein
Positive Selection
dsDNA
5′-Phosphate
Wash
PCR
Remove low-affinity binders
Extract bound DNA with DTT to release Aga2P
B
5′
3′
biotinylated capturing oligo
PE-labeled streptavidin
C
R0
R7
R8
R9
R10
PDGF-A
0%
5%
24%
26%
28%
VEGF
0%
6%
54%
68%
76%
IL-6
5%
6%
5%
9%
12%
Cell Counts
0
10²
10⁴
Fluorescence Intensity

Figure 3-1. Cell-SELEX procedure implemented by ectopic expression of human soluble growth factors on yeast cell surface. (a) A schematic drawing illustrates the procedure for cell-SELEX. Each round consists of subtractive panning, PCR amplification, and recovery of aptamer sequences by lambda exonuclease digestion. Human soluble growth factors were displayed on yeast cell surface as a fusion to agglutinin, composed of Aga1p and Aga2p subunits. Surface expression of the protein of interest was confirmed by antibody binding to hemagglutinin (HA) tag (YPYDVPDYA) and c-myc (EQKLISEEDL) tag. Enrichment and affinity of reactive aptamers to target molecules were quantified by flow cytometry. Selected aptamer pools were subjected to high throughput sequencing to isolate highly enriched sequences. (b) Aptamers for flow cytometry experiments were captured by biotinylated oligonucleotides complementary to either 5' or 3' constant regions. This DNA complex was mixed with PE-conjugated streptavidin at a 1:1 molar ratio. (c) Progressive enrichment of reactive aptamers against PDGF-A, VEGF, and IL-6 were confirmed by flow cytometry. Shown are the binding of aptamers to unrelated proteins (PDGF-B or EGFR) drawn in shaded histograms or to target proteins in open histograms. The percentage of subpopulations defined by arrows is shown for each histogram. Aptamers were used at 200 nM.

Discovery of specific aptamers in accordance with the degree of sequence multiplicity.

Using sequence data obtained from the high-throughput sequencing, I calculated the multiplicity (the number of reads) of the sequences (after accounting for sequencing error by clustering) belonging to the different rounds of SELEX (Table 3-1). I expected a correlation between multiplicity and affinity for aptamers, such that the aptamers with tighter binding to targets are more likely to possess higher multiplicity [24]. I chose for high-throughput sequencing analysis the pools prior to SELEX (round 0) and after rounds 4, 8, 9, and 10; the selected pools from the last three rounds were included as there was a substantial increase in reactive binders measured by flow cytometry (Figure 3-1c). Highly enriched sequences were also tested individually for binding to respective targets by flow cytometry using biotinylated oligonucleotides complementary to the 5' end and PE-conjugated streptavidin (Figure 3-2). For PDGF-A, the top 10 ranked sequences at round 10 accounted for 63% of the total reads with a gradual decrease in multiplicity from top to bottom. In contrast, the top 2 sequences at rounds 8 to 10 for VEGF (named 'hVap1' and 'hVap2') accounted for 80% of the reads, with a dramatic decrease in multiplicity for the remaining sequences. Notably, the gradual decrease in the level of binding for the top three PDGF-A aptamers (named 'hPAap1' to 'hPAap3') (Figure 3-2) was correlated with multiplicity, emphasizing quantitative nature of our flow cytometry-based binding assay.

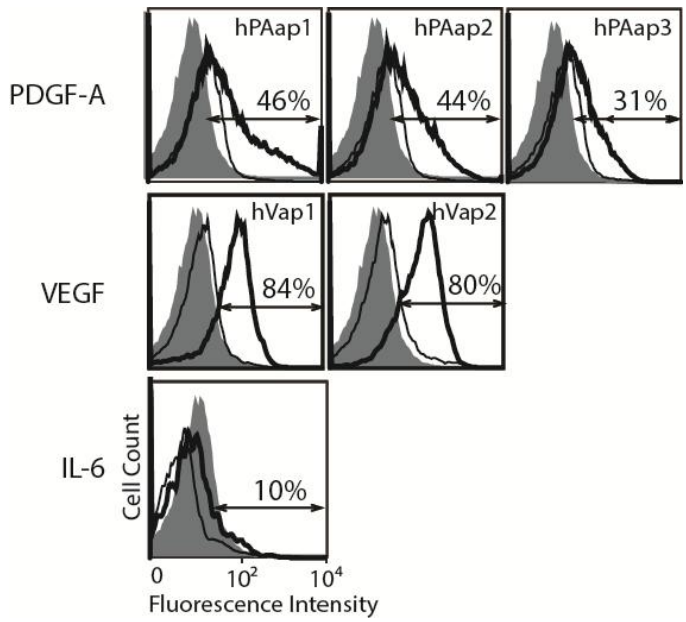

Figure 3-2. Confirmation of binding specificity of the top-ranked aptamers identified by sequence multiplicity. Highly enriched aptamer sequences were identified by high-throughput sequencing analysis, and tested by flow cytometry for specificity and binding affinity to respective targets. The binding of individual aptamers to respective target is shown as open histograms drawn in thick line, to unrelated protein as open histograms in thin line, and to uninduced yeast cells as closed histograms. The percentage of subpopulations defined by arrows is shown for each histogram.

Table 3-1. Enriched aptamer sequences selected against target molecules

Target	Aptamer ID	Sequences of selected aptamers (5'-->3')	Percentage of Total Reads			
			R4	R8	R9	R10
PDGF-A	1	CAGAGCAGGGCGCCGTGTCGCATAGTGTTGTCACTCCCCTGGAGGTCCATGCGAAATATG	0.00	13.66	18.52	12.41
	2	GCGGTATTACCGGGGGCCCTCCGGGTACGATTGGGGCTTCCCTATGCGGATCAGTTGGTA	0.00	7.38	11.00	7.40
	3	CGCCTCTTCTCACCGTGTGAGACTCCACGTCTTGATTGCAGGGTGGTTGCTTCCCATGCG	0.00	1.71	1.57	6.85
	4	GTCGCCAAGGGCCGGGCACTGTCTACCGGTATGGTTTAACCTCCCACGCATAGATCGCGT	0.00	3.14	6.36	6.79
	5	GCTAGGGCCGTCAGGCATAGAACCGTCTATTCAACAGAGGATTCTCCCAGATTCGGTGCG	0.00	15.11	10.02	6.64
	6	GAAACGCCGCTGGGCTAACGGGGGGCCCACAGCGTGGGGACGGTGTTTTGATCTATTCTA	0.00	5.49	11.16	5.64
	7	CTCTGGTCGTGAGCTGGGCGGCTATTGCGTGCTAGCCGGTTACTTTTAGTCCCTAATGCG	0.00	2.94	3.50	5.52
	8	GCGTACGTCTCTCTTCAAGACATGCGGACGGGGGCCCGGTACTACGGGGACGATGTTGCG	0.00	3.78	4.88	5.38
	9	GCTGTGGCACACAGGGGGCCCGCAGGTTTTGCAGCGGGGACGATTACTTTTTCGTGCAG	0.00	20.62	12.00	3.47
	10	AAGTTGTCAGGGCAGGTCGGTTGGGCCAACTTGCATGAGTCATGCTTTCCCCGGCGCTCT	0.00	1.36	2.06	3.24
VEGF	1	TAGCCCACTGCATAGAGGTAGCCACGTATGTGGGTGTTACCCATTCGTAGCTACCGGTGA	0.01	79.91	58.21	31.70
	2	AAAGCCCACTGCATAGAGGCCGCTCAACATGCGAGCCGGTGTACTTCAACAGGTATCCT	0.00	2.60	15.81	48.94
	3	GTGGCTCCGCCCACTGCAAAGAGATGGGGGTATCTTCCATCAGTACCATCATCGGTGTAT	0.00	0.17	1.12	4.18
	4	AATCCCTGGGCGTGCAGCCCCTATTGCGTGCTGCCCACTGCAAAGAACGATAGTGGTGTC	0.00	0.32	1.81	4.14
	5	AGGGTCTTCAGAATTGCTTGGGTCCCCACTGGATAGAGCACAAACTGGGCGGTGCATGAC	0.00	12.80	21.07	4.12
	6	CGGAGATAAGTTAGCCCACTGCAGAGAGGCTCTAGTTTGGCATGCCGTCAAGCCGTTGTT	0.00	0.15	0.77	2.26
	7	ATACGTTGGATCCCACTGAATAGAATTTCGCAGCCTGCTCGAACTGGTGTCGCTAATGTT	0.00	0.06	0.23	0.86
	8	CTTAGTCTACCTAAAACAGCCCACTGCATAGAATCTCGGCTTGTACGAGATGGTTGAACA	0.00	0.01	0.02	0.19
	9	TCTTTCGTGTATAATGGCCCACTGCATAGAGTGACTTGTCATGGTGTTTCCATACTTGGT	0.00	0.01	0.01	0.16
	10	TCCCCACTGGTAAGAGCTTGACAAAGCGGTGTTGTTTCATCTCAGTCTTAACTCTGAGTC	0.00	0.01	0.01	0.02
IL-6	1	TCCCACGCATTCTGCACATCGATACTGAGCATCGTACATGATCCCGCAACGGGCAGTATT	0.00		0.03	0.05
	2	TCCCACGCATTCTGCACATCGCGGTTGGGGGGTAAGTGGGGGGTGGTCAGGGGAGGCGG	0.00		0.01	0.02
	3	TCCCACGCATTCTGCACATCCGGTTTTTGCTCCCATAGTGGACCCTATGTCGGCCCATA	0.00		0.01	0.02
	4	TCCCACGCATTCTGCACATCCTGGCTGCCTCCTAACGCGATCTACTGTTCCAATAGCCAC	0.00		0.01	0.01
	5	TAGCCCACTGCATAGAGGTAGCCACGTATGTGGGTGTTACCCATTCGTAGCTACCGGTGA	0.00		0.03	0.01

Underlined sequences correspond to the conserved sequence motif. Sequences were ranked in the order of highest to lowest percentage of total reads of R10 pools, except the top two sequences in VEGF.

Identification and characterization of aptamers for VEGF.

I then analyzed the highly enriched sequences for the presence of conserved or shared primary (consensus motif) and secondary structures. The top 10 aptamers in round 10 against VEGF were found to contain the consensus motif of [G/C]CCCACTGCA[T/A]AGAG folded into a stem-loop (Figure 3-3a and b), although the position of this motif differed within the variable region (Table 3-1). In contrast, no obvious consensus motifs were found for the PDGF-A aptamers that were present in the majority of the top ranked sequences. As anticipated from the lack of appreciable binding to IL-6 (the binding of the top-ranked aptamer to IL-6 is shown in Figure 3-2), none of the sequences selected against IL-6 reached a multiplicity of 0.1% (Table 3-1). The failure to isolate aptamers against IL-6 is likely due to the lack of high affinity sequences in our starting library, which contained 10^{15} sequences out of a possible diversity of $4^{60} \sim 10^{36}$ for the 60-nt variable region, as well as the nature of IL-6 (isoelectric point (pI) 6.2 compared to 9.5 for PDGF-A and 7.6 for VEGF) being less 'aptogeneic' to nucleic acid aptamers.

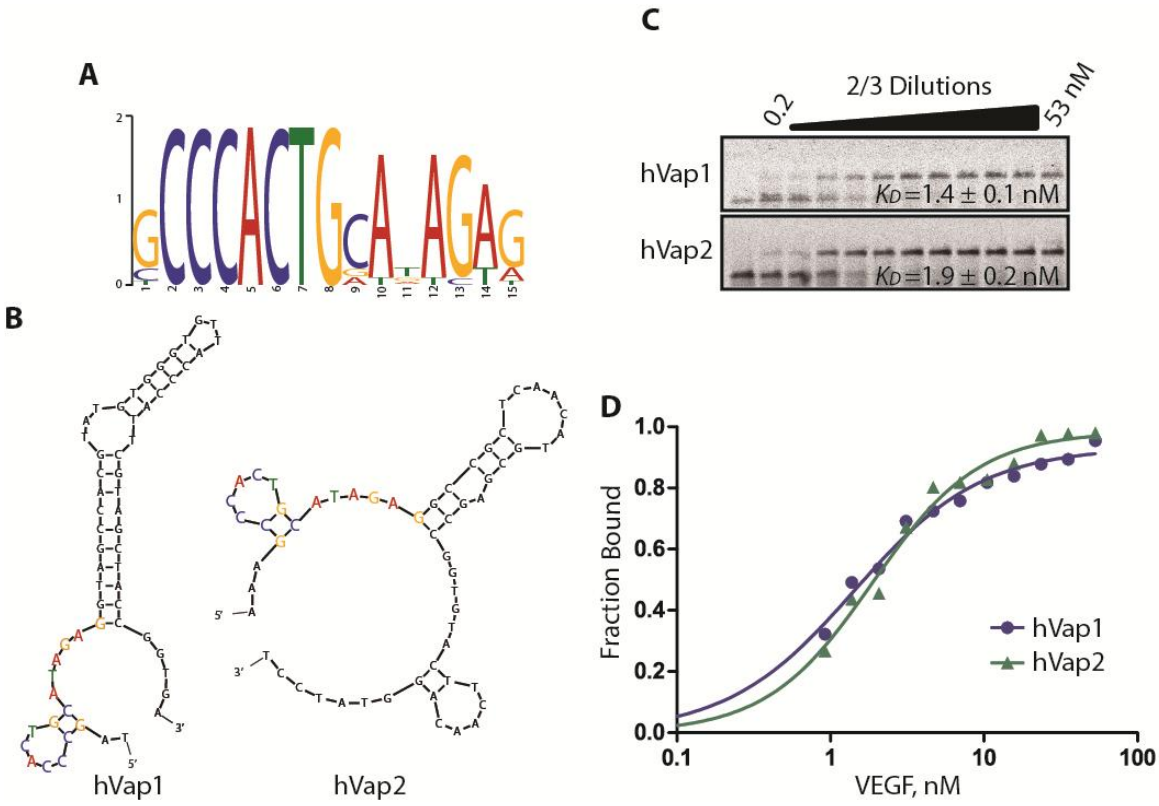

Figure 3-3. Determining consensus motif, secondary structure, and solution affinity of the aptamers against VEGF. (a) The consensus motif shared among the top ten highly enriched sequences against VEGF was identified using the MEME Suite (http://meme.nbcr.net/meme/). (b) Shown are the secondary structures of the 60-nt variable region of the top two aptamers, hVap1 and hVap2, predicted by Mfold (http://mfold.rna.albany.edu/). (c-d) Solution affinity (K_D) of the full-length hVap1 and hVap2 against VEGF was determined by F-EMSA (c), and by fitting the Hill equation to the data (d). VEGF was used at a series of 2/3-fold serial dilutions starting at 53 nM, while labeled aptamers were used at 500 pM.

I then chose the top two ranked aptamers against VEGF to further define solution affinity, structural motif, and their potency as VEGF antagonists. The level of binding to VEGF by hVaps captured by the oligonucleotides complementary to either side of the constant region was equivalent (Supplementary Figure S1), implying that the 20-nt constant region is not a part of the active structure and that the variable region alone is responsible for binding to VEGF. To quantitatively measure the solution affinity of aptamers, I performed a fluorescence electrophoretic mobility shift assay (F-EMSA) using fluorescently-labeled VEGF aptamers [22]. The affinity (equilibrium dissociation constant) of hVap1 and hVap2 against VEGF was measured, respectively, to be K_D = 1.4 ± 0.1 nM and 1.9 ± 0.2 nM (Figure 3-3c and d). In comparison, previously reported DNA aptamers against VEGF bound with much weaker affinity by F-EMSA (K_D = 107.4 ± 9.6 nM for SL12 [25]) or did not exhibit measurable binding (the 25-nt DNA aptamer by Potty et. al., [26]) by flow cytometry when tested under equivalent physiological buffer conditions (Supplementary Figure S2). Both hVap1 and hVap2 were predicted to have the same stem-loop structure comprised of the consensus motif, followed by a longer stem-loop (Figure 3-3b). To further determine if the consensus motif and the predicted secondary structure (Figure 3-3a and b) are the required elements for binding to VEGF, I truncated full-length aptamers into several variants, containing the first stem-loop of the consensus motif and a portion of the adjacent stem-loop (Figure 3-4a and Table 3-2). Again, I performed F-EMSA for each hVap variant and determined the K_D to be 1.7 ± 0.1 nM for hVap1_T1979, 2.5 ± 0.2 nM for hVap1_SST, 5.6 ± 0.3 nM for hVap1_STEM, and 107.4 ± 9.6 nM for hVap2_T2160 (Figure 3-4b and c). Equilibrium dissociation

constants determined by F-EMSA were in close agreement with those estimated from flow cytometry experiments (Supplementary Figure S3), emphasizing simple yet quantitative nature of our assay.

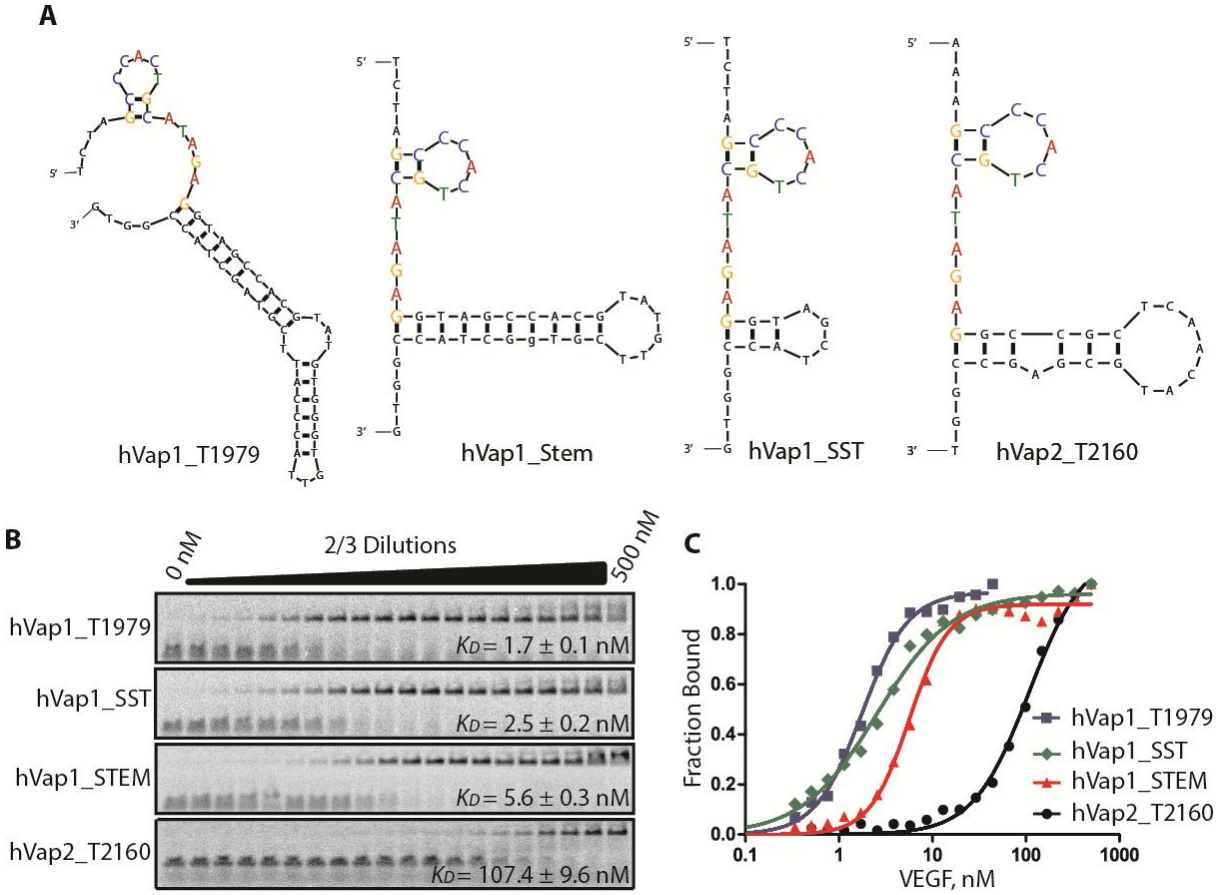

Figure 3-4. Identification of structural motifs of anti-VEGF aptamers. (a) Full-length anti-VEGF aptamers were shortened to contain the first stem-loop containing the consensus motif shared among all highly sequenced aptamers and a part of the longer stem-loop. (b-c) The binding affinities of all four truncated aptamers were determined by F-EMSA assay (b) and by curve-fitting of the Hill equation to the data (c). VEGF was used at a series of 2/3-fold dilutions starting from 500 nM, and labeled aptamers were at 600 pM.

It appears that the first stem-loop in hVap1 is the key structure for binding to VEGF as a significant portion of the second stem-loop could be truncated, applied to hVap1_STEM and hVap1_SST, with less than a 4-fold reduction in binding affinity. Although full-length hVap2 was equally competent as hVap1 in binding VEGF, hVap2_T2160 (hVap2 without a possible third stem-loop (Figure 3-3b)) bound VEGF with ~50-fold reduction in affinity. It is worth mentioning that the 32-nt hVap1_SST, about half the size of hVap1, bound VEGF with a minimum loss in affinity.

Table 3-2. Nucleotide sequences of truncated hVaps

Aptamer Name	Sequences of truncated aptamers (5'->3')	Length (nt)
hVap1_T1979	TCTAGCCCACTGCATAGAGGTAGCCACGTATGTGGGTGTTACCCATTCGTAGCTACCGGTG	61
hVap1_Stem	TCTAGCCCACTGCATAGAGGTAGCCACGTATGT----------TCGTGGCTACCGGTG	48
hVap1_SST	TCTAGCCCACTGCATAGAGGTAGC----------TACCGGTG	32
hVap2_T2160	AAAGCCCACTGCATAGAGGCCGCTCAACATGCGAGCCGGT	40

Dashed lines correspond to the nucleotides that were removed from hVaps. Truncated variants of hVap1 contains 2 nucleotides belonging to the 5' constant region to provide structural flexibility to the variable region when bound with streptavidin. hVap1_Stem contains the first and second stem-loops without the third stem-loop inserted into the second stem-loop. hVap1_SST contains the second stem-loop that is greatly shortened. hVap2_T2160 contains nucleotides 21-60 of the full-length 100-nt hVap2.

Aptamers bind the heparin-binding domain in VEGF.

VEGF is a major regulator of physiological and pathological angiogenesis [27].

VEGF-A or VEGF itself exists in at least seven homodimeric isoforms, of which VEGF165 (the isoform referred to as VEGF herein) is the dominant species, containing both the receptor-binding domain present in all isoforms of VEGF and a heparin-binding domain (HBD) [27]. HBD has been shown to enhance VEGF binding to VEGFR through its interaction with cell-associated heparin-like glycosaminoglycans and sequestration through extracellular heparin molecules [28]. Pegaptanib is known to recognize the HBD in VEGF, and is likely to inhibit VEGF binding to VEGFR-2 in cells [16]. I examined if our aptamers against VEGF could be used as antagonists to VEGF-mediated signalling. With an increasing concentration of hVap2 pre-incubated with soluble VEGF, I observed a gradual decrease in the level of VEGF binding to HeLa cells known to express receptors for VEGF (Figure 3-5a). To further define the structural basis of the inhibition of VEGF binding to VEGFR by our aptamers, I tested if the aptamer binding site is in the receptor binding site or in HBD. When aptamers were tested for binding to VEGF110, devoid of the HBD of VEGF165, all truncated versions of aptamers completely lost the ability to bind VEGF (Figure 3-5b), indicating that the epitope for our aptamers is also within the HBD. However, the preformed complex of VEGF with truncated aptamers, except with hVap2_T2160, could not be reduced by the addition of soluble heparin molecules presumably due to tighter binding of VEGF with the aptamers than with heparin. The decrease in hVap2_T2160 binding to VEGF by heparin is ascribed to its lower affinity binding (K_D = 107 nM). HBDs in human and mouse VEGF are highly conserved (50 identical out of 55 amino acids, shown in Figure 3-5c), which explains the cross-reaction of hVaps with mouse VEGF (Figure 3-5d).

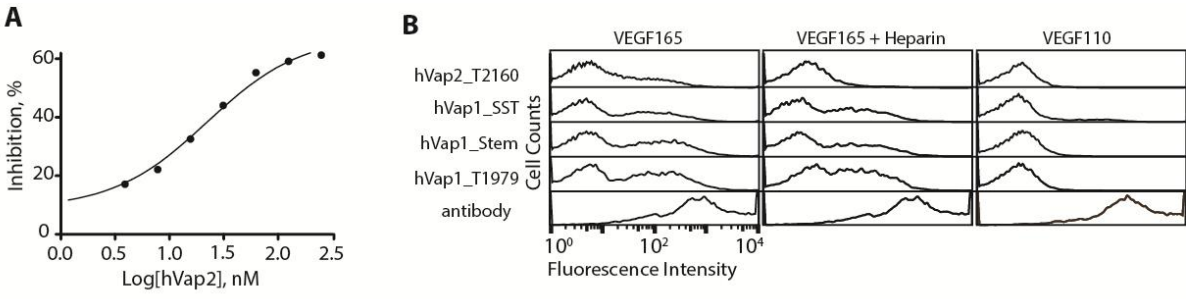

C

Receptor Binding Site

```
1   APMAEGGGQNHHEVVKFMDVYQRSYCHPIETLVDIFQEYPDEIEYIFKPS H
1   APTTEGE-QKSHEVIKFMDVYQRSYCRPIETLVDIFQEYPDEIEYIFKPS M
    **   **   *   *** *********** ************************

51  CVPLMRCGGCCNDEGLECVPTEESNITMQIMRIKPHQGQHIGEMSFLQHN H
50  CVPLMRCAGCCNDEALECVPTSESNITMQIMRIKPHQSQHIGEMSFLQHS M
    ******* ****** ****** *************** ************
```

Heparin Binding Domain

```
101 KCECRPKKDRARQENPCGPCSERRKHLFVQDPQTCKCSCKNTDSRCKARQ H
100 RCECRPKKDRTKPENHCEPCSERRKHLFVQDPQTCKCSCKNTDSRCKARQ M
     *********    ** * ********************************

151 LELNERTCRCDKPRR H
150 LELNERTCRCDKPRR M
    ***************
```

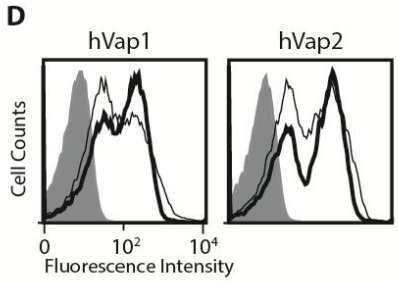

Figure 3-5. Selected aptamers bind the HBD in VEGF. (a) The potency of anti-VEGF aptamers for the inhibition of VEGF binding to VEGFR was measured as the percent inhibition of VEGF binding to VEGFR-expressing HeLa cells. VEGF at 250 nM was pre-incubated with hVap2 at 0 - 250 nM. VEGF binding to cells was detected by polyclonal anti-VEGF antibody. (b) Anti-VEGF aptamers were tested for binding to yeast cells expressing VEGF165 or VEGF110 lacking in HBD with or without post-incubation with 100 nM heparin. Heparin was used to compete with the aptamers for binding to VEGF. VEGF expression was confirmed by polyclonal anti-VEGF antibody. Truncated aptamers were biotinylated at the 5' end to form a complex with PE-conjugated streptavidin. (c) Sequence alignment of human (H) and murine (M) VEGF. '*' indicates identical amino acids between human murine VEGF. Receptor binding domain (residues 1-110 for human VEGF) and heparin binding domain (residues 111-165 for human VEGF) are denoted. (d) Comparison of the level of binding of hVap1 and hVap2 to human (shown in thick open histograms) and murine VEGF (shown in thin open histograms). Aptamer binding to uninduced yeast cells is shown in filled histograms. Aptamers were bound with the biotinylated oligonucleotides complementary to the 5' constant region to form a complex with PE-conjugated streptavidin.

hVaps potently inhibit capillary tube formation of endothelial cells.

Next, using an endothelial capillary tube formation assay, I examined the potency of selected VEGF aptamers for their inhibition of VEGF-mediated endothelial vessel formation. Tube formation assay is a well-defined in vitro assay that has widely been used to screen for angiogenic and anti-angiogenic factors [29], as it reciprocates the process of physiological angiogenesis. HUVECs plated at sub-confluent densities developed complex mesh-like structure patterns when cultured without antagonists, control antibodies, or control ssDNA (Figure 3-6). When treated with bevacizumab (16.6 μM), the HUVECs formed discontinuous but visible sprouting capillary tube patterns. Remarkably, the inhibitory effect of hVaps was more potent with little capillary sprouting patterns, resulting in a reduction of tube length by 60-80% over controls (Figure 3-6b). Therefore, I conclude that our newly selected VEGF aptamers may possess a therapeutic potential for diseases that can be treated or alleviated by anti-angiogenesis therapy.

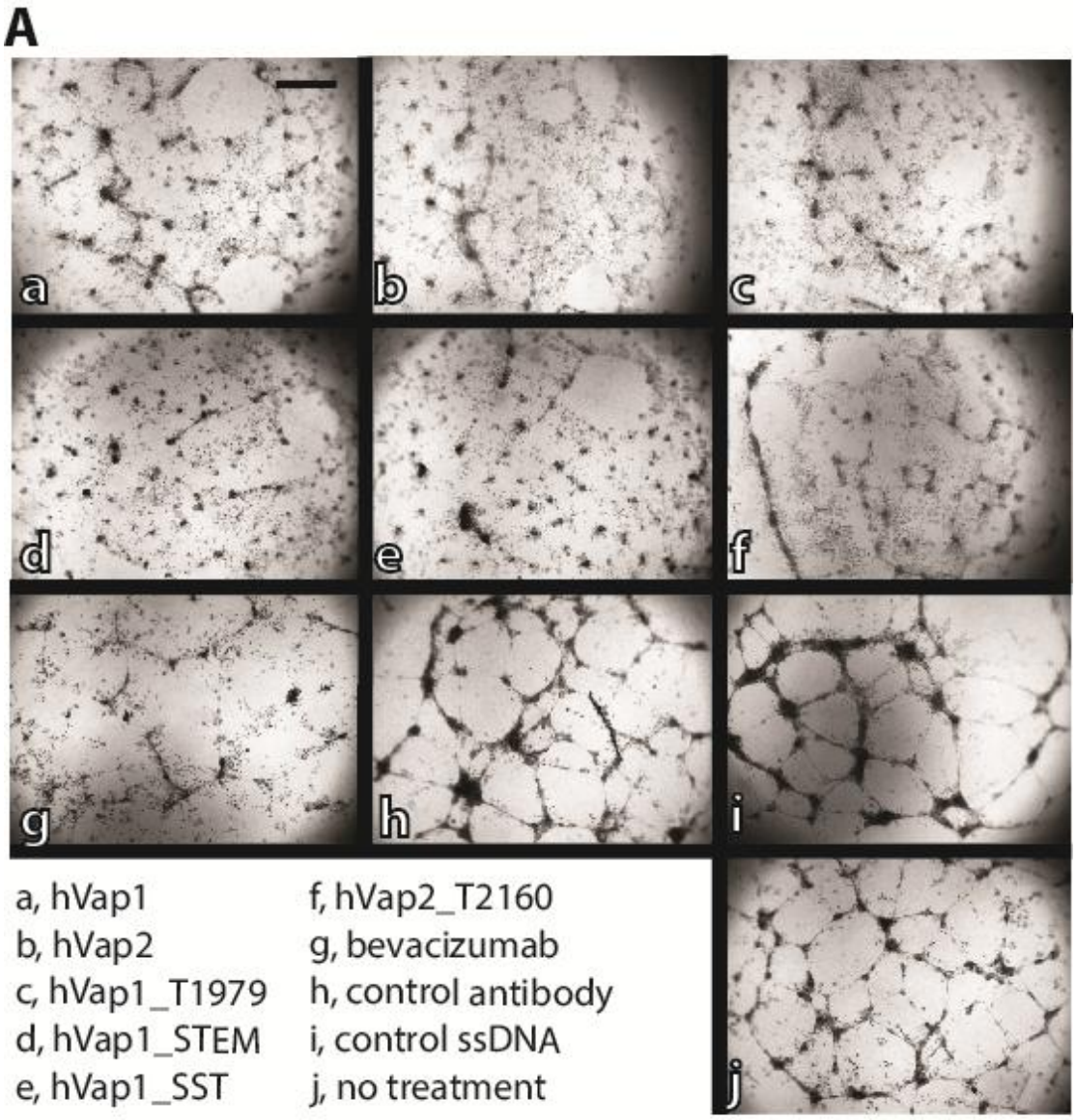
A
a
b
c
d
e
f
g
h
i
j
a, hVap1
b, hVap2
c, hVap1_T1979
d, hVap1_STEM
e, hVap1_SST
f, hVap2_T2160
g, bevacizumab
h, control antibody
i, control ssDNA
j, no treatment
B
Total tube length (µm)
8000
6000
4000
2000
0
a
b
c
d
e
f
g
h
i
j

Figure 3-6. Anti-VEGF aptamers antagonize angiogenesis. Antagonistic potency of anti-VEGF aptamers was measured by a capillary tube formation assay using HUVECs embeded in Matrigel. (a) Shown are the representative images of HUVECs forming capillary tubes after HUVECs were cultured in the presence of anti-VEGF aptamers, bevacizumab, and various controls. Scale bar = 100 μm. (b) Total tube length within a randomly chosen microscopic field (25x magnification) was quantified by Angiogenesis Analyzer for ImageJ software. Bar graph shows the mean and standard deviation of the measured total tube length (n = 3).

Discussion

Serum growth factors are important therapeutic and diagnostic targets, and peptides, antibodies and more recently aptamers have been developed that can detect and antagonize the roles mediated by these growth factors. However, it is challenging to functionally express and immobilize these soluble molecules and to maintain their native conformation through repeated rounds of in vitro selection. Furthermore, conventional methods for determining binding affinity and specificity of candidate aptamers are tedious and incompatible with rapid screening of highly enriched sequences identified by high-throughput sequencing analysis. To address these limitations, I developed a new cell-SELEX approach that circumvents the need for soluble expression, purification, and immobilization of target molecules, and is well-suited for quantitative and rapid screening of candidate aptamers. This is implemented by ectopic expression of soluble growth factors on the cell surface of yeast, and flow cytometry-based assay to quantify binding affinity and specificity of reactive aptamers. The aptamers selected against VEGF using this approach were found to possess high affinity and selectivity, and blocked endothelial tube formation as potently as the monoclonal antibody drug, bevacizumab. Although a number of DNA aptamers against VEGF have been reported, the fact that the aptamers selected in this study are the only high affinity DNA binders in physiological buffer conditions underscore the efficiency of our SELEX strategy.

Compared to the proteins immobilized to planar membranes or polymer beads, the proteins expressed on the yeast cell surface provide an optimal condition for

rapidly depleting non-specific binders and enriching for high affinity binders. This is due to the fact that the library undergoes negative selection with all natively expressed yeast proteins and the positive selection is specific to target protein. Proteins displayed on the surface of yeast cells via a fusion to agglutinin are natively folded, as required to be released through a secretory pathways rather than being degraded intra-cellularly [30]. Furthermore, surface expression of target proteins in living cells should prevent the targets to be non-uniformly displayed to the extent that leads to local clustering or aggregation. This has been recognized as a potential problem as targets immobilized onto planar membranes or beads are prone to selecting non-specific aptamers due to their binding to multiple targets in a cooperative manner [31]. Finally, the net negative charge of the yeast cell wall, composed primarily of polysaccharides, creates a stringent interaction environment for negatively charged nucleic acid aptamers and proteins present on cell surfaces. These conditions are likely responsible for the successful discovery of aptamers against VEGF and PDGF-A as specific and high affinity binders.

High-throughput sequencing analysis of different aptamer pools revealed a quantitative correlation between aptamer multiplicity and binding affinity. Candidate aptamers against VEGF are dominated by the top two ranked aptamers, hVap1 and hVap2, accounting for 80% of the total reads starting from the 8th round SELEX pool. These two aptamers were confirmed to be high affinity binders to VEGF and potent antagonists to VEGF-mediated angiogenesis. Although the 7th round pool was not subjected to high-throughput sequencing, a dramatic increase in the percentage of reactive aptamers from the 7th to the 8th round pool implied that at least 8 rounds of

SELEX were necessary for the discovery of the high affinity aptamers. This corresponds to an enrichment factor of 100-fold per cycle, because the diversity of the starting library is 10^{15}. It is also interesting to note that while hVap1 was dominant from the 8th round, hVap2 progressively enriched from the 8th to the 10th round of SELEX. In contrast, the less pronounced shift of the flow cytometry histogram peaks suggests that aptamers against PDGF-A are weaker binders (with K_D ~ 10-100 nM), which is also reflected in the lack of dominant species revealed by sequence multiplicity. The power of large-scale sequencing for aptamer discovery is also apparent in aptamer pools selected against IL-6. Although flow cytometry revealed gradual enrichment of a reactive population at the 10th round, no single aptamer accounted for more than 1% of the total reads.

The top ranked aptamers by sequence multiplicity accounting for more than 95% reads were found to share the same consensus motif of 15 bases, which adopted a short hairpin structure. Variants of the full-length VEGF aptamers, containing the consensus motif and a truncated form of the adjacent stem-loop, were found to retain almost full capacity binding to VEGF. I speculate that the stem-loop adjacent to the consensus motif may affect binding to VEGF either by direct contact with VEGF or influencing the structure of the consensus motif. The shortest version of the 32-nt VEGF aptamer, consisting of the consensus motif and an adjacent short stem-loop structure, retained affinity to VEGF with less than 2-fold reduction from the full-length 60 nt aptamers. Furthermore, in an endothelial capillary tube formation assay these shortened versions were as potent as the full-length aptamers, which themselves were equally or more effective than the anti-VEGF monoclonal antibody,

bevacizumab. Therefore, the VEGF aptamers developed in this study may find a therapeutic use in diseases whose progression is critically dependent on VEGF-mediated vasculature growth.

Affinity measurement by F-EMSA and flow cytometry demonstrated that the aptamers discovered in this study had higher affinity (K_D < 10 nM) relative to two previously isolated DNA aptamers: 1) SL12, a truncated version of the original 66-nt aptamer that was measured to have K_D = 130 nM and 2) the 25-nt aptamer by Potty et. al., which bound VEGF at a lower affinity with increasing salt concentrations, approaching a μM K_D at physiological conditions. Unlike the reported K_D value of 5 nM for SL12, which was determined by surface plasmon resonance [25], the affinity estimated by our F-EMSA assay was ~100 nM, closer to the affinity of the full-length 66-nt aptamer [32]. The binding of the 25-nt aptamer by Potty et. al. [26] could not be detected by flow cytometry performed under physiological buffer conditions, likely because the detection limit of our assay is K_D ~ 1 μM. Although all these DNA aptamers and the RNA aptamer (pegaptanib) bound VEGF with a wide-range of affinity (sub-nanomolar to micromolar K_D), they all target the HBD, which has a pI of 9 and tends to be a dominant site for interaction with aptamers. One may need to use VEGF devoid of the HBD, such as VEGF110, to isolate aptamers that bind the receptor binding domain to isolate aptamers that can antagonize all isoforms of VEGF.

Overall, the strategy developed in this study, enabling cell-SELEX for selecting aptamers against soluble proteins, rapid enrichment of high affinity and specific binders, and quantitative monitoring of progressive enrichment can be readily extended to the discovery of aptamers against a larger set of antigens. For example,

this can be implemented with multi-well plates and automated fluid-handling systems. The fact that quantitative estimation of the binding affinity between aptamers and target proteins can be achieved by flow cytometry has a significant advantage over conventional methods such as EMSA, which require purified proteins and labelled nucleic acids. Flow cytometry allows a set of yeast cells expressing hundreds of different target proteins to be tested for binding to multiple candidates. Thus, our cell-SELEX platform can facilitate the discovery of high affinity aptamers against a large set of soluble proteins.

SUPPLEMENTARY MATERIALS

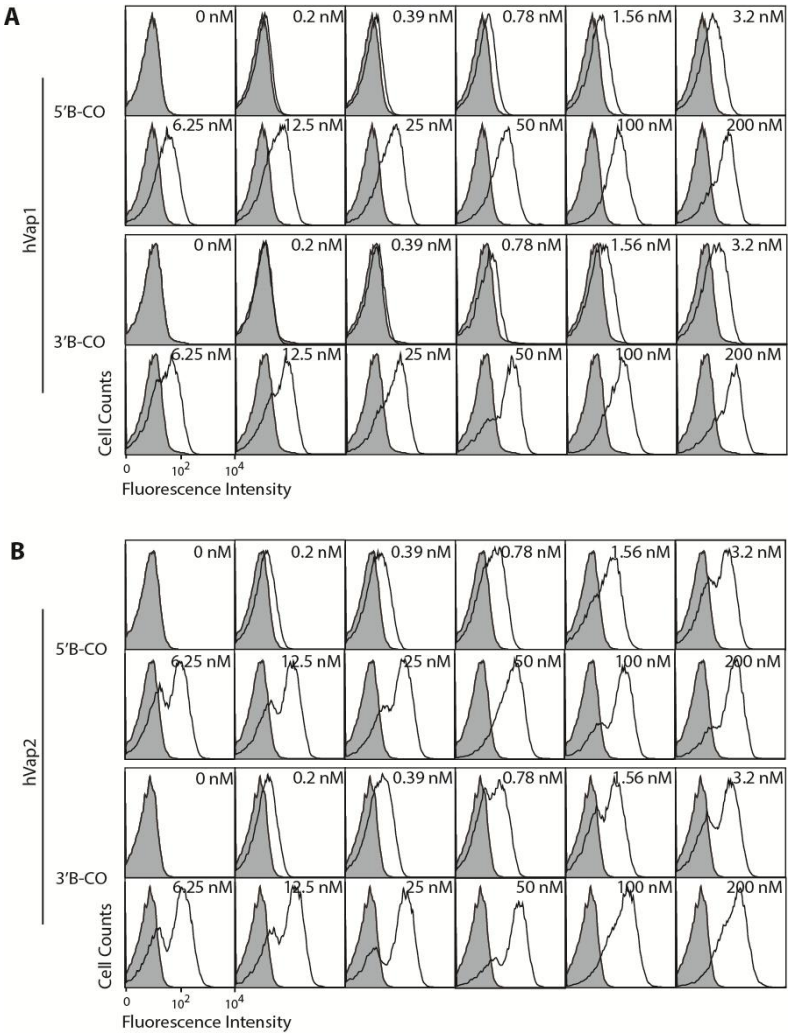

Figure S 1. Constant regions are not part of the active conformation of aptamers. Flow cytometry data are generated with hVap1 (A) and hVap2 (B) aptamers captured with biotinylated oligonucleotides complementary to either 5' (5'B-CO) or 3' constant regions (3'B-CO). The concentration of aptamers used for labeling yeast is indicated for each histogram. Aptamer binding to yeast cells expressing VEGF is shown in open histogram and to uninduced yeast in filled histogram.

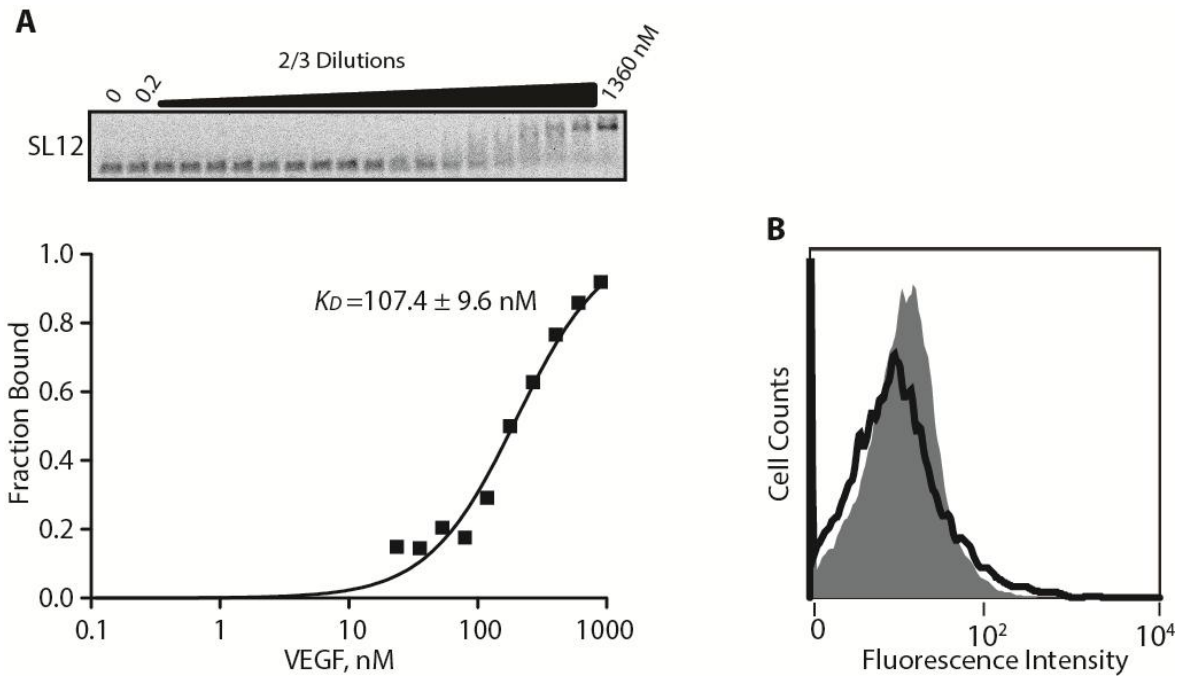

Figure S 2. Binding affinity measurement of previously reported VEGF aptamers. (a) F-EMSA of DNA aptamer SL12 [25] was performed to examine its binding affinity in solution. SL12 was labeled at the 5'-end with fluorescein, used at 500 pM. VEGF was used at a series of 2/3 dilutions ranging from 0 to 1,360 nM. The fraction-bound values were used to determine the dissociation constant (K_D) of SL12 by the Hill equation. (b) Flow cytometry measurement of the binding of the 25-nt aptamer by Potty et. al. to yeast cells expressing VEGF (open histogram) and to uninduced yeast cells (open histogram). The aptamer used at 200 nM for binding was biotinylated at the 5' end to form a complex with PE-conjugated streptavidin.

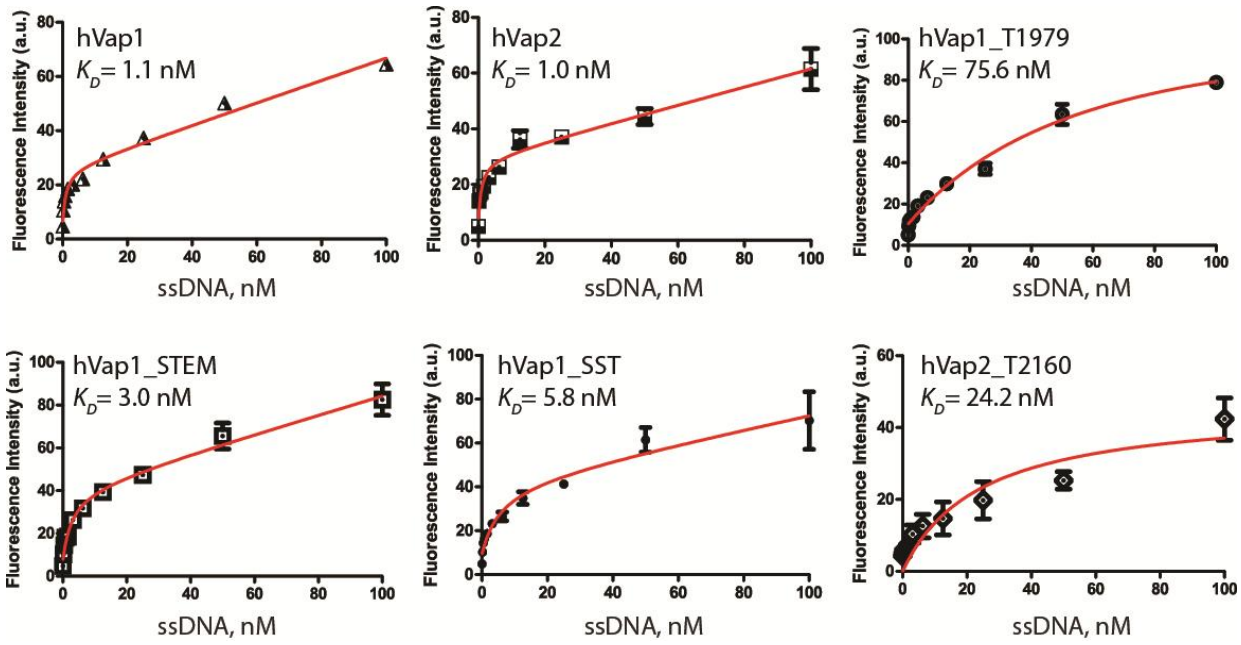

Figure S 3. Measuring binding affinity of truncated aptamers to VEGF by flow cytometry. Aptamers were used at 0 – 100 nM. Data points are mean ± standard deviation from duplicate experiments.

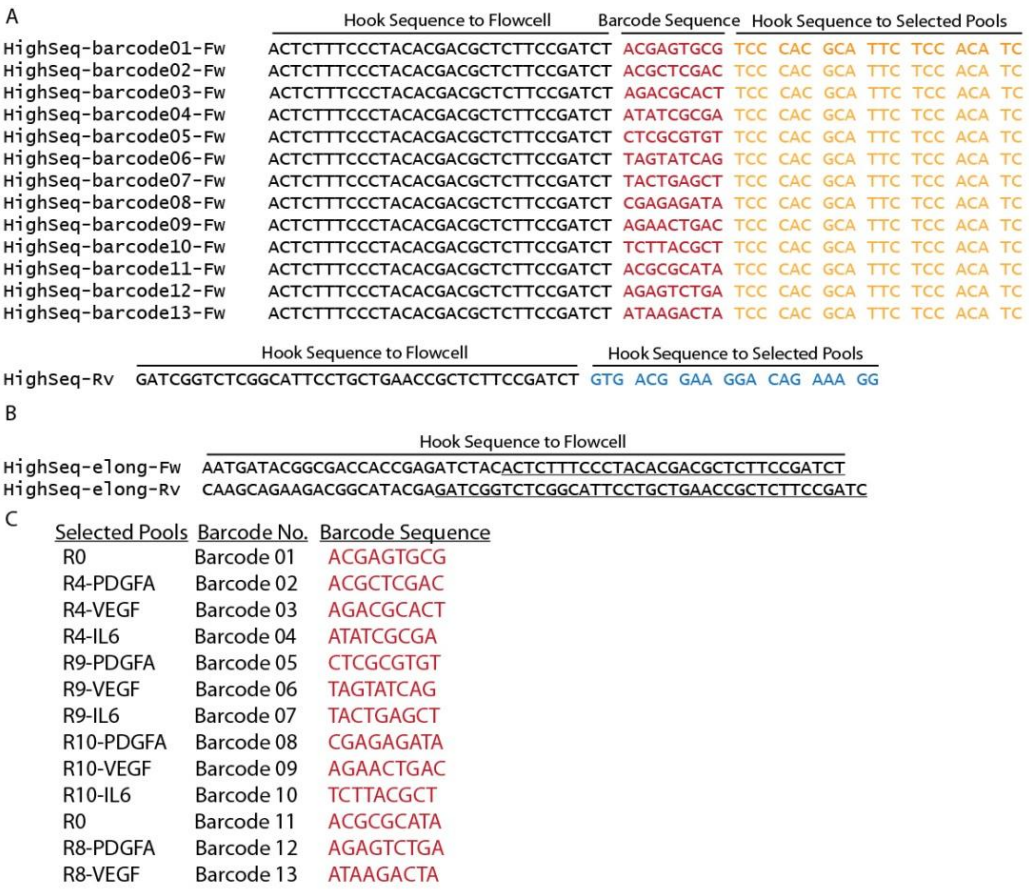

Figure S 4. The primer set of selected pools for high-throughput DNA sequencing by the HiSeq 2000 (Illumina). (a) Primer set; forward primers: with adaptors to the flowcell and to the DNA, barcodes for each chosen-selected pools; reverse primer: with adaptors to the flowcell and to the DNA. (b) Both forward and reverse primers are further sequences for the adaptors to the flowcell. (c) Each barcode was subjected to a selected pool to differentiate. I first took a small portion of selected DNA pools and performed PCR with primers in (a). After clean-up, I then performed PCR with the primer set in (b).

REFERENCES

1. Jenison, R.D., et al., *High-resolution molecular discrimination by RNA.* Science, 1994. **263**(5152): p. 1425-9.
2. Patel, D.J., et al., *Structure, recognition and adaptive binding in RNA aptamer complexes.* J Mol Biol, 1997. **272**(5): p. 645-64.
3. Wecker, M., D. Smith, and L. Gold, *In vitro selection of a novel catalytic RNA: characterization of a sulfur alkylation reaction and interaction with a small peptide.* RNA, 1996. **2**(10): p. 982-94.
4. Joyce, G.F., *Amplification, mutation and selection of catalytic RNA.* Gene, 1989. **82**(1): p. 83-7.
5. Ellington, A.D. and J.W. Szostak, *In vitro selection of RNA molecules that bind specific ligands.* Nature, 1990. **346**(6287): p. 818-22.
6. Tuerk, C. and L. Gold, *Systematic evolution of ligands by exponential enrichment: RNA ligands to bacteriophage T4 DNA polymerase.* Science, 1990. **249**(4968): p. 505-10.
7. Shangguan, D., et al., *Aptamers evolved from live cells as effective molecular probes for cancer study.* Proc Natl Acad Sci U S A, 2006. **103**(32): p. 11838-43.
8. Rose-John, S. and P.C. Heinrich, *Soluble receptors for cytokines and growth factors: generation and biological function.* Biochem J, 1994. **300 (Pt 2)**: p. 281-90.

9. Krueger, J.G., et al., *Role of growth factors, cytokines, and their receptors in the pathogenesis of psoriasis.* J Invest Dermatol, 1990. **94**(6 Suppl): p. 135S-140S.

10. Ferrara, N., et al., *Discovery and development of bevacizumab, an anti-VEGF antibody for treating cancer.* Nat Rev Drug Discov, 2004. **3**(5): p. 391-400.

11. Levitzki, A., *Targeting signal transduction for disease therapy.* Curr Opin Cell Biol, 1996. **8**(2): p. 239-44.

12. Nakahara, H., et al., *Anti-interleukin-6 receptor antibody therapy reduces vascular endothelial growth factor production in rheumatoid arthritis.* Arthritis Rheum, 2003. **48**(6): p. 1521-9.

13. Gold, L., et al., *Aptamer-based multiplexed proteomic technology for biomarker discovery.* PLoS One. **5**(12): p. e15004.

14. Hu, X., et al., *Combinatorial libraries against libraries for selecting neoepitope activation-specific antibodies.* Proc Natl Acad Sci U S A, 2010. **107**(14): p. 6252-7.

15. Gschwind, A., O.M. Fischer, and A. Ullrich, *The discovery of receptor tyrosine kinases: targets for cancer therapy.* Nat Rev Cancer, 2004. **4**(5): p. 361-70.

16. Ng, E.W., et al., *Pegaptanib, a targeted anti-VEGF aptamer for ocular vascular disease.* Nat Rev Drug Discov, 2006. **5**(2): p. 123-32.

17. Holash, J., et al., *VEGF-Trap: a VEGF blocker with potent antitumor effects.* Proc Natl Acad Sci U S A, 2002. **99**(17): p. 11393-8.

18. Gragoudas, E.S., et al., *Pegaptanib for neovascular age-related macular degeneration.* N Engl J Med, 2004. **351**(27): p. 2805-16.

19. Chomczynski, P. and N. Sacchi, *Single-step method of RNA isolation by acid guanidinium thiocyanate-phenol-chloroform extraction.* Anal Biochem, 1987. **162**(1): p. 156-9.

20. Boder, E.T. and K.D. Wittrup, *Yeast surface display for screening combinatorial polypeptide libraries.* Nat Biotechnol, 1997. **15**(6): p. 553-7.

21. Latulippe, D.R., et al., *Multiplexed microcolumn-based process for efficient selection of RNA aptamers.* Anal Chem, 2013.

22. Zearfoss, N.R. and S.P. Ryder, *End-labeling oligonucleotides with chemical tags after synthesis.* Methods Mol Biol, 2012. **941**: p. 181-93.

23. Avci-Adali, M., et al., *Upgrading SELEX technology by using lambda exonuclease digestion for single-stranded DNA generation.* Molecules, 2010. **15**(1): p. 1-11.

24. Cho, M., et al., *Quantitative selection of DNA aptamers through microfluidic selection and high-throughput sequencing.* Proc Natl Acad Sci U S A, 2010. **107**(35): p. 15373-8.

25. Kaur, H. and L.Y. Yung, *Probing high affinity sequences of DNA aptamer against VEGF165.* PLoS One, 2012. **7**(2): p. e31196.

26. Potty, A.S., et al., *Biophysical characterization of DNA aptamer interactions with vascular endothelial growth factor.* Biopolymers, 2009. **91**(2): p. 145-56.

27. Ferrara, N., H.P. Gerber, and J. LeCouter, *The biology of VEGF and its receptors.* Nat Med, 2003. **9**(6): p. 669-76.

28. Krilleke, D., et al., *Molecular mapping and functional characterization of the VEGF164 heparin-binding domain.* J Biol Chem, 2007. **282**(38): p. 28045-56.

29. Arnaoutova, I., et al., *The endothelial cell tube formation assay on basement membrane turns 20: state of the science and the art.* Angiogenesis, 2009. **12**(3): p. 267-74.

30. Ellgaard, L. and A. Helenius, *Quality control in the endoplasmic reticulum.* Nat Rev Mol Cell Biol, 2003. **4**(3): p. 181-91.

31. Platt, M., et al., *Aptamer evolution for array-based diagnostics.* Anal Biochem, 2009. **390**(2): p. 203-5.

32. Hasegawa, H., K. Sode, and K. Ikebukuro, *Selection of DNA aptamers against VEGF165 using a protein competitor and the aptamer blotting method.* Biotechnol Lett, 2008. **30**(5): p. 829-34.

CHAPTER 4

CONCLUSIONS AND FUTURE DIRECTIONS

Conclusions

I have developed a yeast-cell-based technology for the efficient selection of nucleic acid aptamers for multiple targets in parallel. Our yeast-cell SELEX has a number of advantages over other methods of SELEX processes. First, our yeast-cell SELEX system utilized the advantage of yeast surface display to mobilized target proteins at the yeast cell surface. This character greatly simplified the protein purification steps compared to other methods of SELEX. The platform of yeast surface display expresses proteins through endoplasmic reticulum (ER) with proper protein folding and modifications that unfolded proteins be retained in the reticulum. Second, yeast-cell SELEX also offers a great advantage with east to monitor the selection enrichment and progression throughout the entire SELEX. By examining the binding events between yeast targets and selected pools through flow cytometry, data set can be facile to generate and analyze the enrichments and progressions of selected pools during SELEX. Last but not the least, the yeast surface is negatively charged, and the aptamer pools (DNA or RNA) are also negatively charged. The aptamers that got enriched and selected from yeast-cell SELEX are usually with very tight binding affinity maybe due to these aptamers having conquered the natural repelling force caused by the interaction of yeast cell surface and the aptamer pool.

For this study, I focused on the selection of DNA aptamers; however, our approach would also work for RNA aptamers. I sought to discover DNA aptamers against human serum markers for potential therapeutic and diagnostic applications. To circumvent soluble expression and immobilization for performing SELEX, I ectopically expressed soluble growth factors on the surface of yeast cells to enable cell-SELEX and devised a flow cytometry-based method to quantitatively monitor progressive enrichment of specific aptamers. By applying high-throughput sequencing of selected pools, I revealed that the emergence of highly enriched sequences concurred with the increase in the percentage of reactive aptamers shown by flow cytometry. Particularly, selected DNA aptamers against VEGF were specific and of high affinity (K_D = ~ 1 nM), and demonstrated a potent inhibition of capillary tube formation of endothelial cells, comparable to the effect of a clinically approved anti-VEGF antibody drug, bevacizumab. Considering the fact that many mammalian secretory proteins have been functionally expressed in yeast, the strategy of implementing cell-SELEX and quantitative binding assay can be extended to discover aptamers against a broad array of soluble antigens.

Future Directions

Since the fact that many mammalian secretory proteins can be functionally expressed in yeast, the strategy of expanding and implementing cell-SELEX and quantitative binding assay can be extended to discover aptamers against a broad array of soluble antigens. In order to reach this goal, I will further carry out a comprehensive design of experiments to conduct yeast-cell SELEX systematically in a 96-well or 386-

well plate. The advantage here is that yeast-cell SELEX provides a panel of aptamers with diverse characteristic with regards to their interactions with several different kinds of proteins not just with soluble ones. Afterwards, a potentially constitutive biomarker library for disease treatment, detections and diagnosis can be established.

After specific aptamers have been identified, Surface Plasmon Resonance based Biacore will be applied to validate each aptamer's binding affinity and specificity. Necessary affinity maturations will be issued to some aptamers to increase their affinity, but affinity maturation is not required if there are aptamers with high affinity.

Aptamer as imaging probes.

One of the ongoing and interesting designs of applications for the generated library is aptamer-conjugated moieties as molecular probes for tumor imaging. Tumor imaging is to identify tumor properties and growth, and in a long run, to monitor treatment and treat the tumor. Molecular imaging (MI) has made a significant impact on the field of oncology and is playing an increasingly important role in the diagnosis and treatment of cancer, through clinical applications, research and drug development. Conventional molecular probes typically require a waiting period of hours following injection to allow the probe to distribute to target tissues and for excess probe to exit the body before an imaging procedure. Despite that washout period, low levels of unbound probe remain in the body during the imaging procedure and decrease contrast and sensitivity[1]. To improve contrast, molecules such as antibodies and peptides have been engineered to activate via enzyme processing upon target binding to produce a signal[2]. However, these molecules need to undergo a series of modifications to decrease immunogenicity;

antibodies also are bulky molecules that take time to clear from the body[3] though conformational changed aptamers upon binding to their target have been designed[4].

To synthesize and design an aptamer probe for imaging, a thorough understanding of aptamer binding motif is needed. For imaging purpose, a targeted binding moiety can be designed. Carriers suitable for multimodality including both imaging and therapeutic intervention, include protein scaffolds, specifically streptavidin and avidin, which have been approved for clinical trial, and demonstrate superior diffusion through interstitial space compared to that of rigid spherical particles of comparable size. To synthesize a multi-versatile activatable aptamer-conjugated moiety, taking the advantage of four binding sites to biotinylated molecules of a tetrameric streptavidin molecule will be an efficient design. The primary goal of the design is to utilize the incorporation of aptamer probe and streptavidin to stabilize the whole complex and prevent degradation during manipulations. Furthermore, the complex can increase the avidity of aptamer probes to target, and streptavidin can be fluorescently labeled if the labeling site at the aptamer is not ideal. Ultimately, four different binding sites of a streptavidin can be loaded not just with aptamer probes but also with different payloads for further applications.

Aptamer as therapeutics

Aptamers can be selected from libraries of random sequence oligonucleotides to bind a various range of proteins with affinities and specificities that are comparable to antibodies. Unlike antibodies, aptamers are easier to be created, less immunogenic, and more economical to synthesize. Despite these advantages, aptamer have been slow to reach the marketplace with only one aptamer-based drug[5] that's been approved and

applied clinically so far. Some aptamers that are being developed have great potential to expand the society with a different option for clinical treatments. Aptamers can be used for therapeutic purpose in the same way as antibodies, but with easier approaches to be developed and produced. Very like monoclonal antibodies[6], aptamers can theoretically be used therapeutically in any disease for which extracellular blockade of protein-protein interactions is required. In general, nuclease-mediated degradation is the challenge for aptamers work as a drug. So far, some SELEX experiments for therapeutic use oligonucleotides that are chemically modified [7-10].

During my studies with yeast-cell SELEX for isolating aptamers, I realized the pivotal role of a successful selection of great aptamers for therapeutic purposes is truly relying on how target proteins are expressed and displayed to expose its ligand binding sites/ important domains for aptamer selections.

The aptamer gets selected against the important ligand binding site may have phenomenal role for disease treatments.

REFERENCES

1. Hong, H., et al., *Molecular imaging with nucleic acid aptamers.* Curr Med Chem, 2011. **18**(27): p. 4195-205.
2. Kobayashi, H., et al., *Rational chemical design of the next generation of molecular imaging probes based on physics and biology: mixing modalities, colors and signals.* Chem Soc Rev, 2011. **40**(9): p. 4626-48.
3. Goldenberg, D.M., et al., *Cancer Imaging and Therapy with Bispecific Antibody Pretargeting.* Update Cancer Ther, 2007. **2**(1): p. 19-31.

4. Shi, H., et al., *Activatable aptamer probe for contrast-enhanced in vivo cancer imaging based on cell membrane protein-triggered conformation alteration.* Proc Natl Acad Sci U S A, 2010. **108**(10): p. 3900-5.

5. Ng, E.W., et al., *Pegaptanib, a targeted anti-VEGF aptamer for ocular vascular disease.* Nat Rev Drug Discov, 2006. **5**(2): p. 123-32.

6. Nissim, A. and Y. Chernajovsky, *Historical development of monoclonal antibody therapeutics.* Handb Exp Pharmacol, 2008(181): p. 3-18.

7. Biesecker, G., et al., *Derivation of RNA aptamer inhibitors of human complement C5.* Immunopharmacology, 1999. **42**(1-3): p. 219-30.

8. Ruckman, J., et al., *2'-Fluoropyrimidine RNA-based aptamers to the 165-amino acid form of vascular endothelial growth factor (VEGF165). Inhibition of receptor binding and VEGF-induced vascular permeability through interactions requiring the exon 7-encoded domain.* J Biol Chem, 1998. **273**(32): p. 20556-67.

9. Burmeister, P.E., et al., *Direct in vitro selection of a 2'-O-methyl aptamer to VEGF.* Chem Biol, 2005. **12**(1): p. 25-33.

10. Gold, L., et al., *Aptamer-based multiplexed proteomic technology for biomarker discovery.* PLoS One, 2010. **5**(12): p. e15004.

APPENDIX 1

PROTEIN ENGINEERING TO ENGINEERED B1 INTEGRIN I-LIKE DOMAIN WITH FUSION OF SINGLE-CHAIN IGG-FC INTO A HIGH-STABILITY FORM, ANCHORD-I-LIKE DOAMIN, FOR DELIVERY PURPOSE

Summary

Integrins are non-covalently associated αβ heterodimeric cell surface receptors that mediate cell-cell and cell-extracellular matrix adhesions[1], signaling bidirectionally across the plasma membrane[2]. Intercellular adhesion molecule-1 (ICAM-1) is the ligand for αLβ2 integrin (lymphocyte function associated antigen-1; LFA-1). The intermolecular binding interaction of these two molecules happens within the single domains called α I domain of the integrin and the first domain (D1) at the N-terminal domain of ICAM-1. I previously engineered the I domain into high affinity while preserving the native sequence in the C-terminal α7-helix, whose downward displacement is linked to allosteric activation of integrins[3].

Integrins play important roles in development, immune cell trafficking and responses, and homeostasis. In recent years, great progress has been made towards targeting integrins in cancer treatment, and clinical studies with various integrin inhibitors have demonstrated their effectiveness in blocking cancer progression. It will be valuable to investigate Integrin inhibitor such as DNA aptamers for contributing the

society a potentially new path for cancer drug.

This appendix describes the preliminary results and analyses of β1 anchored-I domain engineering for its potential application to work as a target for yeast-cell SELEX and a fusion to human ScFc-IgG_1 for the carrier of a tool of drug delivery. The anchored-I domain from β1 integrin subunit, in this appendix, was engineered by stability design and validated through yeast surface display system. The final goal of this study has been to use the engineered high affinity anchored-I domain as a platform to develop function-blocking inhibitors, therapeutic aptamers that specifically or preferentially antagonize the active conformation of β1 integrins.

Introduction and Significance

ICAM-1 (Intercellular Adhesion Molecule 1) also known as CD54 (Cluster of Differentiation 54) is a protein that in humans is encoded by the ICAM1 gene.[4] This gene encodes a cell surface glycoprotein which is typically expressed on endothelial cells and cells of the immune system. It binds to integrins of type CD11a / CD18, or CD11b / CD18 and is also exploited by rhinovirus as a receptor. The intercellular adhesion molecule (ICAM) 1 is an Ig-like cell adhesion molecule expressed by several cell types, including leukocytes and endothelial cells. It can be induced in a cell-specific manner by several cytokines, for example, tumor necrosis factor-alpha (TNF-α), interleukin-1(IL-1), and interferon-gamma(IFN-γ), and inhibited by glucocorticoids. Its ligands are the membrane-bound integrin receptors LFA-1 and Mac-1 on leukocytes, CD43, the soluble molecule fibrinogen, the matrix factor

hyaluronan, rhinoviruses, and Plasmodium falciparum malaria-infected erythrocytes. ICAM-1 expression is predominantly transcriptionally regulated. ICAM-1 plays an important role in inflammatory processes and in the T-cell mediated host defense system. It functions as a costimulatory molecule on antigen-presenting cells to activate MHC class II restricted T-cells, and on other cell types in association with MHC class I to activate cytotoxic T-cells. ICAM-1 on endothelium plays an important role in migration of (activated) leukocytes to sites of inflammation. ICAM-1 may play a pathogenetic role in rhinovirus infections. Derangement of ICAM-1 expression probably contributes to the clinical manifestations of a variety of diseases, predominantly by interfering with normal immune function. Among these diseases, most of them are malignancies (e.g., melanoma and lymphomas), such as many inflammatory disorders (e.g., asthma and autoimmune disorders), atherosclerosis, ischemia, certain neurological disorders, and allogeneic organ transplantation. Interference with ICAM-1 leukocyte interaction using mAbs, soluble ICAM-1, antisense ICAM-1 RNA, and in the case of melanoma mAb-coupled immunotoxin, may offer therapeutic possibilities in the future. Integration of knowledge concerning membrane-bound and soluble ICAM-1 into a single functional system is likely to contribute to elucidating the immunoregulatory function of ICAM-1 and its pathophysiological significance in various disease entities[5].

Previously, I have engineered the I domain into a high binding-affinity version, F265S/F292G mutants of LFA-1 I domains (Id-HA) [3], and were able to successfully purify the protein by getting it expressed in E. coli BL21 (DE3) (Novagen), refolded, and purified as previously described[6]. I also noticed the purified Id-HA showed fast

degradation after purification. In this report, I have documented the preliminary results and analyses of the newly engineering Id-HA, β1 anchored-I domain (AncId-HA), for its potential application to work as a target for yeast-cell SELEX and a fusion to human Sc-Fc-IgG_1 for the carrier of a tool of drug delivery.

Experimental Procedures

Transfection

The day before transfection, 1–3 × 10^5 cells in complete growth medium were prepared in each 35-mm dish and incubated at 37℃ (5% CO_2) overnight. Cells were grown 50–80% confluent before transfection after overnight incubation. For each 35-mm dish to be transfected, 100 µl serum-free medium (Advanced DMEM) were placed into a sterile tube. 3 µl GeneJuice® Transfection Reagent were added dropwise directly to the serum-free medium, mixed thoroughly by vortexing, and incubate at room temperature for 5 min. For each 35-mm dish to be transfected, 1 µg DNA were added to GeneJuice reagent/serum-free medium mixture and mixed by gentle pipetting. Afterwards, GeneJuice reagent/DNA mixture was incubated at room temperature for 5–15 min. The entire volume of GeneJuice reagent/DNA mixture were added drop-wise to cells in complete growth medium and dispersed drops over entire surface of dish followed by incubating cells for 24–72 h at 37℃ (5% CO_2). Analyze cells after harvest.

Immunofluorescence Flow Cytometry.

Antibodies used in this study were the anti-c-Myc antibody 9E10 (ATCC), rh-ICAMI-Fc (R&D), and phycoerythrin-labeled goat polyclonal anti-murine antibodies (Santa Cruz Biotechnology). After induction, yeast cells were harvested, washed in 100 μl of the labeling buffer (PBS containing 0.5% BSA with 10 mM $MgCl_2$ or 10 mM EDTA), and then incubated with ligands in 50 μl of the labeling buffer for 20 min with shaking at 30 ℃. Cell were then washed and incubated with secondary antibodies at 5 μg⁄mL in 50 μl of the labeling buffer for 20 min at 4 °C. Finally, cells were washed once in 100 μl and suspended in 100 μl of the labeling buffer for flow cytometry (Epics XL flow cytometer, Beckman Coulter).

Results

The design of Anchored-I domain

AncId-HA, the new version of Id-HA, was designed to complement the stability of the purified protein of Id-HA (F265S/F292G) and serve as a potential target of yeast-cell SELEX. In an effort to create a tool for drug delivery and characterize the newly-design protein, two versions of Id-HA were designed (Fig. 1). In the design, I replaced the 311 Glycine with a Cystein and extended five amino acids at the N-terminal from the original Id-HA to create AncId-HA. From the design, the high-affinity binding of the Id-HA to ICAMI-I had been maintained and also the virtue of having a hypothetical disulfide bond could also stabilize the α7-helix in an open position.

a <Fc-AncId-HA>

MDMRVPAQLLGLLLLWFPGSRCHHHHHHEPKSCDKTHTCPPCPAPELLGGPSVFLFPPKPKDTLMISRTP
EVTCVVVDVSHEDPEVKFNWYVDGVEVHNAKTKPREEQYNSTYRVVSVLTVLHQDWLNGKEYKCKVSNKA
LPAPIEKTISKAKGQPREPQVYTLPPSRDELTKNQVSLTCLVKGFYPSDIAVEWESNGQPENNYKTTPPV
LDSDGSFFLYSKLTVDKSRWQQGNVFSCSVMHEALHNHYTQKSLSLSPGKGGGGSGGGGSECIKGNVDLV
FLFDGSMSLQPDEFQKILDFMKDVMKKLSNTSYQFAAVQFSTSYKTEFDFSDYVKRKDPDALLKHVKHML
LLTNTFGAINYVATEVFREELGARPDATKVLIIITDGEATDSGNIDAAKDIIRYIIGIGKHFQTKESQET
LHKFASKPASEFVKILDTFEKLKDLFTELQKKIYVIECTS*

b<Anc-Id-HA>

ECIKGNVDLVFLFDGSMSLQPDEFQKILDFMKDVMKKLSNTSYQFAAVQFSTSYKTEFDFSDYVKRKDPD
ALLKHVKHMLLLTNTFGAINYVATEVFREELGARPDATKVLIIITDGEATDSGNIDAAKDIIRYIIGIGK
HFQTKESQETLHKFASKPASEFVKILDTFEKLKDLFTELQKKIYVIECTS*

Figure A-1. Characterizations of I domain fusion proteins.

(a&b) Single letter amino acid sequences and domain demarcations of the fusion proteins, Fc-AncId-HA (a) and AncId-HA (b).

Characterization of Fc-AncId-HA protein in mammalian-cell system

To test if the newly design Fc-AncId-HA can be functionally expressed in mammalian-cell system, I have constructed the fusion proteins into vector pHIV-EGFP and transfected the DNA with GeneJuice® Transfection Reagent (EMD Millipore) to Hela cells to observe the characterizations of the proteins. After transfection, the fluorescent intensity of EGFP protein was observed and indicated that the Fc-AncId-HA protein was expressed and folded properl and functionally (Figure A-2a). Furthermore, I also constructed the newly designed AncId-HA to vector pNL6 and expressed the protein through YSD system as previously described[7] to examine the binding affinity of AncId-HA to ICAMI in detail. Preliminary, AncId-

HA showed no binding to CD11 alpha Antibody (TS1/22) when wildtype Id and previously engineering αL Id-HA[8] show significant binding (Figure A-3). TS1/22 was mapped to the ligand binding region of the αL domain (residues Gln-266 and Ser-270) and competitively inhibits αLβ2 [9, 10]. A possible explanation to the lack of binding of TS1/22 to AncId-HA could be the hypothetical disulfide bond has slight alternate the steric binding mechanism of TS1/22 to αL domain- (residues Gln-266 and Ser-270) but still maintain the binding capability of AncId-HA to ICAM-I (Figure A-3).

A quick comparison of binding affinity in both Id-HA and AncId-HA has been performed based on previously described method. Due to the conformation of Id-HA and AncId-HA expressed in yeast, the yeast cells can bind to Hela cells (Figure A-2b). By comparing the yeast binding capacity to Hela cells can have a quick scan for distinguishing the binding affinity of AncId-HA and Id-HA to ICAM-I. From the result (Figure A-2b), AncId-HA yeast showed almost comparable but slight higher numbers of yeast cells binding to Hela cells than Id-HA, which indicated AncId-HA may have tighter binding affinity than Id-HA to ICAM-I.

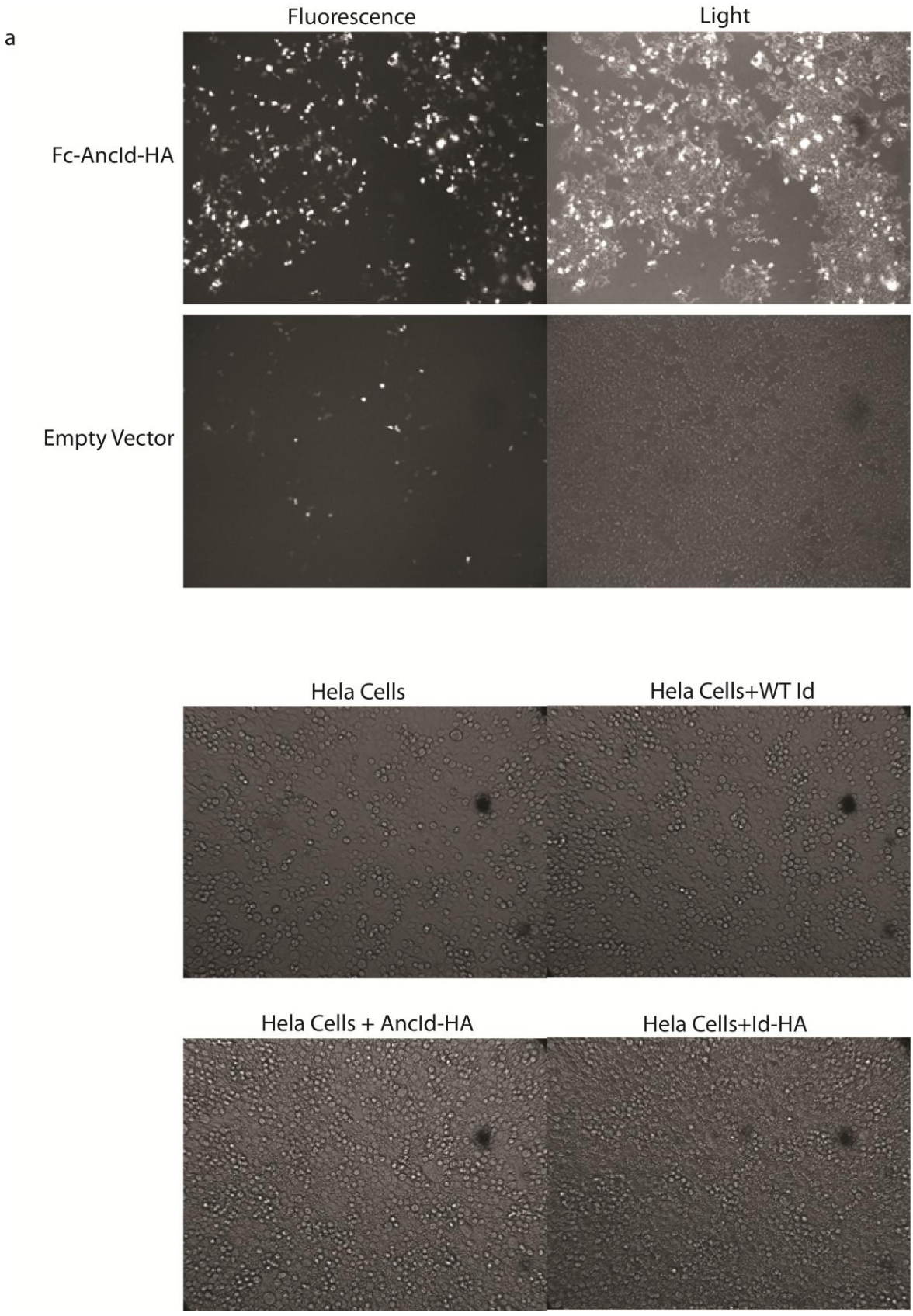
a
Fluorescence
Light
Fc-AncId-HA
Empty Vector
Hela Cells
Hela Cells+WT Id
Hela Cells + AncId-HA
Hela Cells+Id-HA

Figure A-2. Newly engineered AncId-HA can be functionally expressed in mammalian cell system and in yeast-surface display system. (a). Fc-AncId-HA was constructed in vector pHIV and successfully expressed in Hela cells with the fusing EGFP expressed. (b) AncId-HA was constructed in vector pNL6, and the yeast cells show binding interaction with Hela cells. Yeast cells appear as small bright spheres in the images.

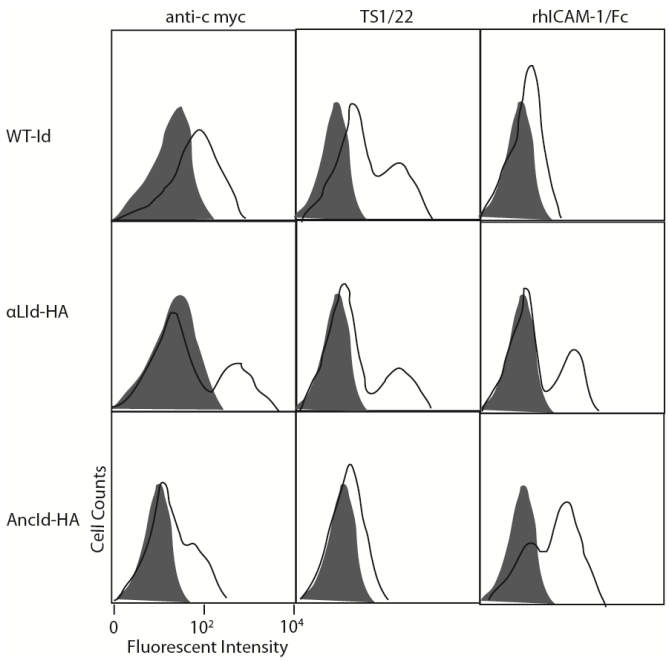

Figure A-3. Comparison of binding affinity to ICAM-I. Wildtype Id yeast, αL Id-HA yeast, and AncId-HA yeast were used to test the binding with 9E10, TS1/22, and rhICAM-1/Fc. Though AncId-HA yeast didn't show binding to TS1/22, it shows the strongest binding to rhICAM-1/Fc.

Discussion

In murine xenograft models, mAbs directed against tumor-specific antigens largely remain in the blood and no more than 20% of the administered dose typically interacts with the tumor[11]. This represents probably one of the major limitations faced by mAbs. Antibody uptake by the tumor depends on a subtle balance between favourable pharmacokinetics and efficient penetration and retention in the targeted tissue, and various characteristics of mAbs, such as molecular size, shape, affinity and

valency control these properties. mAbs are large molecules that are characterized by very long serum half-lives. They far exceed the renal clearance threshold (<70 kDa), preventing them from being eliminated through the kidney glomeruli. Moreover, the Fc portion of IgG molecules can interact with various receptors expressed at the surface of several cell types, which increase their retention in the circulation. Most importantly, the Fc portion can interact with the neonatal Fc receptor (FcRn) expressed at the surface of several cell types, including vascular endothelium cells, monocytes and macrophages as well as with barrier sites such as the blood–brain interface, the glomerular filter in the kidneys and the intestinal epithelium[12]. Based on the preliminary results, more binding affinity assay can be performed to identify the binding affinity to ICAM-1. After being fully characterized, the Fc-AncId-HA protein can be purified through mammalian system and establish the method for adding payloads to the Fc portion to achieve the goal of targeting delivery.

REFERENCES

1. Springer, T.A. and J.H. Wang, *The three-dimensional structure of integrins and their ligands, and conformational regulation of cell adhesion.* Adv Protein Chem, 2004. **68**: p. 29-63.
2. Hynes, R.O., *Integrins: bidirectional, allosteric signaling machines.* Cell, 2002. **110**(6): p. 673-87.
3. Jin, M., et al., *Directed evolution to probe protein allostery and integrin I domains of 200,000-fold higher affinity.* Proc Natl Acad Sci U S A, 2006. **103**(15): p. 5758-63.
4. Katz, F.E., et al., *Chromosome mapping of cell membrane antigens expressed on activated B cells.* Eur J Immunol, 1985. **15**(1): p. 103-6.
5. van de Stolpe, A. and P.T. van der Saag, *Intercellular adhesion molecule-1.* J Mol Med (Berl), 1996. **74**(1): p. 13-33.
6. Owens, R.M., et al., *Engineering of single Ig superfamily domain of intercellular adhesion molecule 1 (ICAM-1) for native fold and function.* J Biol Chem, 2010. **285**(21): p. 15906-15.
7. Boder, E.T. and K.D. Wittrup, *Yeast surface display for screening combinatorial polypeptide libraries.* Nat Biotechnol, 1997. **15**(6): p. 553-7.
8. Shimaoka, M., et al., *Reversibly locking a protein fold in an active conformation with a disulfide bond: integrin alphaL I domains with high affinity and antagonist activity in vivo.* Proc Natl Acad Sci U S A, 2001. **98**(11): p. 6009-14.

9. Lu, C., et al., *The binding sites for competitive antagonistic, allosteric antagonistic, and agonistic antibodies to the I domain of integrin LFA-1.* J Immunol, 2004. **173**(6): p. 3972-8.

10. Lu, C., et al., *Locking in alternate conformations of the integrin alphaLbeta2 I domain with disulfide bonds reveals functional relationships among integrin domains.* Proc Natl Acad Sci U S A, 2001. **98**(5): p. 2393-8.

11. Beckman, R.A., L.M. Weiner, and H.M. Davis, *Antibody constructs in cancer therapy: protein engineering strategies to improve exposure in solid tumors.* Cancer, 2007. **109**(2): p. 170-9.

12. Roopenian, D.C. and S. Akilesh, *FcRn: the neonatal Fc receptor comes of age.* Nat Rev Immunol, 2007. **7**(9): p. 715-25.